General Solutions for Magnetohydrodynamics Flow of a Viscoelastic Fluid through Porous Medium

By

BUSHRA RIAZ

NATIONAL UNIVERSITY OF MODERN LANGUAGES

ISLAMABAD

APRIL, 2025

General Solutions for Magnetohydrodynamics Flow of a Viscoelastic Fluid through Porous Medium

By

BUSHRA RIAZ

MS MATH, National University of Modern Languages, Islamabad, 2025

A THESIS SUBMITTED IN PARTIAL FULFILMENT OF

THE REQUIREMENTS FOR THE DEGREE OF

MASTER OF SCIENCE

In **Mathematics**

To

FACULTY OF ENGINEERING & COMPUTING

NATIONAL UNIVERSITY OF MODERN LANGUAGES ISLAMABAD

NATIONAL UNIVERSITY OF MODERN LANGUAGES FACULTY OF ENGINEERING & COMPUTER SCIENCE

THESIS AND DEFENSE APPROVAL FORM

The undersigned certify that they have read the following thesis, examined the defense, are satisfied with overall exam performance, and recommend the thesis to the Faculty of Engineering and Computing for acceptance.

Thesis Title: General Solutions for Magnetohydrodynamics Flow of a Viscoelastic Fluid through Porous Medium

Submitted By: Bushra Riaz **Registration #:** 65 MS/MATH/F22

Master of Science in Mathematics (MS MATH)
Title of the Degree

Mathematics
Name of Discipline

Dr. Asia Anjum
Name of Research Supervisor

Signature of Research Supervisor

Dr. Sadia Riaz
Name of HOD (MATH)

Signature of HOD

Dr. Muhammad Noman Malik
Name of Dean (FE&C)

Signature of Dean (FE&C)

Date: 17th April, 2025

AUTHOR'S DECLARATION

I Bushra Riaz

Daughter of Raja Riaz Ahmed

Registration # 65 MS/MATH/F22

Discipline Mathematics

Candidate of **Master of Science in Mathematics (MS MATH)** at the National University of Modern Languages do hereby declare that the thesis **General Solutions for Magnetohydrodynamics Flow of a Viscoelastic Fluid through Porous Medium** submitted by me in partial fulfillment of MS MATH degree, is my original work, and has not been submitted or published earlier. I also solemnly declare that it shall not, in future, be submitted by me for obtaining any other degree from this or any other university or institution. I also understand that if evidence of plagiarism is found in my thesis/dissertation at any stage, even after the award of a degree, the work may be cancelled and the degree revoked.

Signature of Candidate

Bushra Riaz

Name of Candidate

17th April, 2025

Date

ABSTRACT

Title: General Solutions for Magnetohydrodynamics Flow of a Viscoelastic Fluid through Porous Medium

In this thesis, a theoretical investigation is undertaken for simple Couette flow and acceleration flow for non-Newtonian fluid. Exactly, we establish exact solution for the fully developed unsteady laminar flows of an incompressible hydromagnetic Maxwell fluid h lies between two parallel plates. One of the plate is stationary while the other plate moves with the velocity $Uf(t)$, where $f(t) = H(t)$ or $f(t) = H(t)t^a(a > 0)$. Also, the effect of porous medium is taken into account and the constant pressure is applied in the direction of the flow. The analytical solution for the velocity field, shear stress and the volume flux are obtained in simple form by means of finite Fourier sine transform. These solution, depending on the initial and boundary condations are presented as a sun of steady and transient solutions. Furthermore, the solutions for Newtonian fluid performing the same motion are also obtained for simple Couette flow and the accelerating flows are also obtained as limiting cases for our general solution. Finally, the effect of the material parameters on the velocity profile and shear stress are spotlighted by means of the graphical illustration.

TABLE OF CONTENTS

LIST OF FIGURES

LIST OF ABBREVIATIONS

FFST	-	Finite Fourier Sine Transform
PDE	-	Partial Differential Equation
ODE	-	Ordinary Differential Equation
ASBL	-	Asymptotic Suction Boundary Layer

LIST OF SYMBOLS

u, v	-	Velocity components in x and y directions
D/Dt	-	Upper convective time derivative
d/dt	-	Material time derivative
∇	-	Gradient
ρ	-	Fluid density
μ	-	Coefficient of dynamic viscosity or viscosity
p	-	Pressure
A	-	Amplitude
λ	-	Maxwell parameter
τ	-	Shear stress
Re	-	Reynolds number
$\boldsymbol{T}$	-	Cauchy stress tensor
t	-	Time
We	-	Weissenberg number
K	-	Porosity parameter
$\boldsymbol{I}$	-	Identity tensor
$\boldsymbol{V}$	-	Velocity vector
$\boldsymbol{S}$	-	Extra-stress tensor
U	-	Amplitude of the velocity
$\boldsymbol{A}_1$	-	First Rivlin-Ericksen tensor
$u_{Fs}(t)$	-	Finite Fourier Sine Transform of $u(y,t)$
r_{1n}, r_{2n}	-	Roots
K_{eff}	-	Effective permeability
F_b	-	Lorentz force
$\boldsymbol{R}$	-	Darcy resistant
ν	-	Kinematic viscosity
$\boldsymbol{L}$	-	Velocity gradient
φ	-	Permeability

M	-	Dimensionless magnetic parameter
$Q(t)$	-	Volume flux
k	-	Permeability
F_x	-	x-component of Body force

ACKNOWLEDGMENT

I wish to express my gratitude and deep appreciation to Almighty Allah, who made this study possible and successful. I am speechless when it comes to expressing my warm appreciation to the Almighty Allah, who is the most forgiving and helpful to all of creation. I also thank Hazrat Prophet Muhammad (PBUH), the final prophet of the Almighty Allah, who is regarded as the world's greatest reformer and human educator. First and foremost, I want to express my sincere gratitude to Dr. Asia Anjum, my supervisor, for her unwavering support, tolerance, and vast knowledge. She provided great advice at every turn during the research and writing process. I would like to thank my parents deeply for their prayers, constant support, encouragement, and gratitude. Their presence has served as a constant source of inspiration and strength. I want to sincerely thank everyone who helped and advised me while I was doing this research. Finally, I want to sincerely thank my sisters and friends for their support during my MS degree path. (Bushra Riaz)

DEDICATION

This thesis work is dedicated to my parents and my teachers throughout my education career who have not only loved me unconditionally but whose good examples have taught me to work hard for the things that I aspire to achieve.

CHAPTER 1

INTRODUCTION AND LITRATURE REVIEW

1.1 Non-Newtonian Fluid

Newtonian fluid provides ease of theoretical modeling because of their constant viscosity, which is independent of shear stress or strain rate. Nevertheless, a large number of fluids seen in practical applications are non-Newtonian, with viscosities that change in response to pressure, time, or shear rate. Because of their non-linear behavior and requirement for mathematical techniques like fractional calculus or non-linear differential equations, non-Newtonian fluids such as those controlled by power-law viscosity-pressure dependencies present considerable difficulties.

The flow of a second-grade incompressible fluid over a porous plate was examined by Rajagopal *et al*. [1], who looked into suction and blowing solutions. In contrast to classical Newtonian behavior, their results showed that the presence of solutions is strongly influenced by the material moduli. The pressure-dependent viscosity in flows between parallel plates was also read by Fetecau *et al*. [2], who provided solutions for shear stress and velocity under time-dependent bottom plate motion. These investigations highlighted how important viscosity differences are in defining flow properties.

Asif *et al*. [3] used Fourier integral transformations to model shear stresses in non-Newtonian (Brinkman) flows driven by oscillatory shear forces. They emphasized the distinctions between non-Newtonian and Newtonian behaviors in these kinds of flows. These studies were expanded to unstable, compressible second-grade fluids by Rajagopal *et al*. [4], who examined time-periodic Poiseuille flow and oscillating plate-induced flows.

1.2 Maxwell Fluid

Maxwell fluids combine the characteristics of a fluid and a solid, exhibiting viscoelastic qualities. Because of these features, stylish mathematical techniques are required to take strain-rate dependency and stress relaxation into consideration. Differential equations that describe how a fluid reacts to time-dependent forces are frequently used in accurate solutions. Oscillatory Maxwell fluid flow in triangular tubes was studied by Sun *et al*. [5], who derived velocity and phase difference formulae impacted by Deborah numbers and relaxation time. Wenchang *et al*. [6] demonstrated the adaptability of this method by modeling unsteady Maxwell fluid flows between plates, driven by impulsive and periodic motions, using fractional calculus.

The effects of magnetic fields, relaxation parameters, and oscillation frequencies on Maxwell fluid flows close to semi-infinite plates were examined by Bao *et al*. [7]. Stability under absorbing boundary circumstances was highlighted in their findings. In order to examine heat and mass transfer in Maxwell fluids, Riaz *et al*. [8] created fractional differential operators, such as the Atangana-Baleanu derivative, and demonstrated their benefits over conventional derivatives. Together, these investigations showed how important fractional calculus and numerical methods are for simulating Maxwell fluids.

1.3 Magnetohydrodynamic (MHD)

MHD integrates fluid dynamics and electromagnetism principles to study how electrically conducting fluids behave in magnetic fields. Electric currents are produced when fluid velocity and magnetic fields interact, which has an impact on heat transfer and flow stability.

Zheng *et al*. [9] used fractional calculus to evaluate and generate solutions for MHD flows of Oldroyd-B fluids caused by accelerating plates. Their results provided information on Maxwell fluids and generalized second-grade fluids under magnetic forces. This work was expanded to dusty fluids in boundary layer flows by Jalil *et al*. [10], who focused on skin friction and magnetic field-induced velocity variations.

Rehman *et al*. [11] in Newtonian and non-Newtonian fluids, investigated revealed that cylindrical planes outperform them in relations of heat transfer rate and temperature regime. These advantages are further enhanced by magnetic fields, which advance our knowledge of the thermophysical aspects of flow fields. Analytical solutions for Maxwell fluids in porous media were presented by Fetecau *et al*. [12] and [13], who emphasized the impact of porous materials on steady-state behavior and slower flow rates in comparison to Newtonian fluids.

1.4 Porous Medium

The study of fluid flow in porous media is vital for applications such as filtration, groundwater flow, and enhanced oil recovery. The interaction between fluid properties and porous structures introduces additional complexities, requiring advanced mathematical modeling.

Hassan *et al*. [14] explored nanofluid flows in porous media, demonstrating that nanoparticle concentration enhances convection heat transfer, while porous interactions reduce it. Krishna *et al*. [15] analyzed MHD convective flows over inclined plates in porous media, emphasizing ion slip and Hall effects. Yang *et al*. [16] examined water-alumina oxide nanofluids in wavy porous media, highlighting the impacts of electromagnetic fields and entropy formation on heat transfer. These studies underscore the importance of porous structures in modifying flow and thermal behaviors, with implications for energy and environmental systems.

1.5 Couette Flow

Viscosity and boundary layer phenomena can be fundamentally understood using the Couette flow model, which is the shear flow between two parallel plates. Wall transpiration, oscillatory wall motion, and dipolar fluids have all been added to its scope in recent studies.
When Jordan *et al*. [17] examined unstable Couette flow of dipolar fluids under fast top plate motion, they discovered backflows and discontinuities in velocity. Wall slip effects were examined by Khaled *et al*. [18], who discovered that excessive slip lessens transients in Couette flow and decreases oscillation amplitudes and transients in Stokes flow.
In their explicit solutions for inhomogeneous shear flows, Ershkov *et al*. [19] showed counterflows and vorticity distributions in Couette flow. Sun *et al*. [20] investigated boundary-

layer transitions to the asymptotic suction boundary layer (ASBL) and critical Reynolds numbers in Couette flow with continuous wall transpiration.

1.6 Contribution to Thesis

The work is extended to investigate the MHD Maxwell fluid flow in the presence of a porous material with particular initial and boundary conditions, after the review study by Fetecau *et al*. [21] is detailed. Using the integral transform, exact analytical solutions are found for two scenarios: simple couette flow and flow caused by an accelerating plate. Mathematica and MATLAB applications are used to learn the graphical behaviors of several relevant parameters.

1.7 Thesis Organization

These are the structure of the remaining thesis:

Chapter 1 gives an overview of the main ideas as well as an introduction to the thesis.

Chapter 2 gives some basic definitions used in the study to obtain numerical findings for the flow problem.

Chapter 3 discusses in detail the general solutions for hydromagnetic flow of viscous fluids between horizontal parallel plates through porous medium by Fetecau, *et al*. [21].

Chapter 4 provides extended work based on Fetecau, *et al*. [21].

Chapter 5 concludes by discussing the complete research process and the possible future uses of this finding.

References a list of the references consulted for this thesis can be found in the Bibliography.

CHAPTER 2

Fundamental and Basic Definitions

2.1 Fluid

A fluid is a material that flows and conforms to the shape of its cylinder. It contains both liquids and gasses. Fluids are distinguished by their ease of movement and features such as viscosity (flow resistance) and hydrostatic pressure (uniform pressure exerted in all directions). They are essential in many natural processes and industry, including transportation, engineering, and medicine, see [22].

2.1.1 Special Qualities of Fluids

- **Hydrostatic pressure**: Fluids can apply pressure uniformly in all directions.
- **Viscosity**: The flow resistance of a fluid.
    - Fluids vary in viscosity (thick/high viscosity vs. thin/low viscosity).

2.1.2 Applications of Fluids

- Fluids are critical in:
    - Engineering, transportation, weather forecasting, and medical fields.
    - Processes such as blood circulation, hydraulic systems, cooling systems, and weather patterns.

2.2 Newtonian Fluid

The viscosity of a Newtonian fluid remains constant regardless of the force or stress applied to it. This implies that its flow behavior remains constant even when pressure or stress levels vary, see [22].

Examples:

- Water
- Air
- Oil
- Alcohol

2.3 Non-Newtonian Fluid

A non-Newtonian fluid is one whose viscosity varies as stress or force is applied. Non-Newtonian fluids, as opposed to Newtonian fluids, have a variable viscosity Dr. R.K. Bansal. [22]

Examples:

- **Ketchup**: Becomes thinner (flows more easily) when shaken or squeezed (shear-thinning).
- **Toothpaste**: Stays thick in the tube but flows when squeezed out (shear-thinning).
- **Blood**: Acts as a non-Newtonian fluid as its flow characteristics change under different conditions.

2.4 Compressible Fluid

A compressible fluid is one whose density varies affectedly under pressure. Gases are usually compressible fluids because their molecules are widely apart and may be pressed closer together under pressure.

Example:

- air
- helium
- natural gas

Application:

- Compressible fluids are important in aerodynamics, gas pipelines, and engines because pressure fluctuations affect performance.

2.5 Incompressible Fluid

An incompressible fluid is one whose density remains almost constant even while under pressure. Most liquids are considered incompressible because their molecules are densely packed and resistant to further compression.

Examples:

- water
- oil
- most liquids

Application:

- Incompressible fluids are frequently assumed in hydraulic systems, fluid dynamics, and civil engineering to simplify computations.

2.6 Types of Flow

2.6.1 Steady Flow

A system is said to be in steady flow when the fluid properties remain consistent throughout time at any given point. Stated differently, flow properties such as temperature, pressure, and velocity don't change over time at a certain location. Think about a river whose flow rate is constant. Selecting a specific location in the river and tracking the water's characteristics over time will reveal that they remain constant, see [23].

2.6.2 Unsteady Flow

In unsteady flow, flow characteristics such as temperature, pressure, density, and velocity change over time, unlike steady flow, which has continuous fluctuations, see [24].

Examples:

- Gusty breeze
- Ocean waves and tsunamis
- Arteries' blood flow
- Unstable rocket aerodynamics

2.6.3 Incompressible Flow

Incompressible flow maintains a constant density independent of pressure changes. This indicates that the volume of the fluid constituents remains constant, even when pressure or temperature changes. Under normal conditions, liquids such as water are commonly thought to be incompressible. In circumstances with modest flow speeds and moderate pressure fluctuations, the density remains almost constant, simplifying fluid dynamics calculations. [25]

2.6.4 Laminar Flow

Laminar flow is an effect of fluid particles move smoothly and orderly in parallel strata with little mixing between layers. When fluid particles move in laminar flow along clearly defined paths, there is minimal or no turbulent motion, see [26].

2.7 Viscosity

A fluid's resistance to the force that causes it to flow is known as its viscosity. In simple terms, it determines a fluid's internal friction. Kinematic viscosity, apparent viscosity, relative viscosity, and dynamic (absolute) viscosity are among the several forms of viscosity.

Examples:

- **Honey:** High viscosity, flows slowly.
- **Water:** Low viscosity, flows quickly.
- **Motor oil:** Medium viscosity, varies with temperature.

2.8 Porous Medium

A material is considered a porous medium if it contains a continuous form and many communicated pores. Because the substance's pores are filled with fluid, the fluid can leave. There are many different shapes and sizes of pores in a porous medium. Whether a medium such as dry bread, wood, beach sand, sandstone or is porous is determined by its porosity.

2.8.1 Porosity

The medium porosity is the ratio of the entire area of a material to its related void area. It is characterized by φ. As a result, the substance's section. Porosity is defined as the proportion of linked voids to total volume. When all pore space is not linked, such as in sponges, wood, rubber, and some rocks, this is referred to as effective porosity.

2.8.2 Permeability

Permeability refers to a material's ability to enable fluids to flow through it. It measures the ease with which water or other fluids may flow through porous materials such as soil or rock. High permeability suggests that fluids may flow freely, whereas low permeability shows that fluid movement is limited. It is essential for applications such as groundwater movement, oil extraction, and environmental engineering

2.8.3 Darcy's Law

Darcy's Law describes the movement of fluids through a porous media. It asserts that the flow rate is directly proportional to the pressure differential across the medium and conversely proportional to the fluid's viscosity and the medium's resistance.

$$\boldsymbol{q} = \frac{-K}{\mu} \boldsymbol{\nabla} p, \tag{2.1}$$

where $\boldsymbol{\nabla} p$ is pressure drop, μ is the dynamic viscosity , K is Porosity parameter and $\boldsymbol{q}$ is the instantaneous flow rate.

2.9 Continuity Equation

The law of mass conservation, known as the continuity equation, states that the entrance mass of a system is equal to the sum of its exit mass and the internally developed entry mass. The equation for continuity is expressed as follows:

$$\frac{\partial \rho}{\partial t} + \boldsymbol{\nabla}.(\rho \boldsymbol{V}) = 0, \tag{2.2}$$

where $\boldsymbol{V}$ is the velocity and ρ the density of fluid. For incompressible fluid,

$$\boldsymbol{\nabla}.\boldsymbol{V} = 0. \tag{2.3}$$

2.10 Momentum Equation

The momentum equation, which is based on Newton's second law of motion, compares the sum of forces exerted on the fluid component with its increase in velocity or momentum transformation. Incompressible fluids have a particular equation of movement:

$$\rho \frac{d\boldsymbol{V}}{dt} = \boldsymbol{\nabla}.\boldsymbol{T} - \rho \boldsymbol{b} \tag{2.4}$$

where $\frac{d}{dt}$ the upper convective derivative, ρ is density, $\boldsymbol{T}$ is Cauchy stress tensor , $\boldsymbol{b}$ the body force .

2.11 Integral Transforms

To determine the initial point of an integral transform, the Fourier integral formula was frequently used. Integral transformations have been used in applied mathematics and engineering research to solve numerous difficulties. An integral transform is a one-of-a-kind mathematical process for transforming to convert an actual or complex-valued function into an additional function. The integral transform's foremost purpose is to make a complex mathematical problem easier to understand so that it can be resolved quickly and directly without the need for complicated and lengthy computations. It has been demonstrated that integral transformations are effective methods for resolving linear differential equations, initial boundary value issues, and initial value difficulties of integrals. These problems typically arise whereas investigating issues related to fluid mechanics, see [27].

2.12 Finite Fourier Sine Transform

The finite fourier sine transform is a sort of fourier transform that expresses a function specified over a limited interval with sine functions. It is widely used to solve problems with specified boundary conditions, such as heat conduction or wave equations, in which the function disappears at the borders.

Formula:

For a function $f(x)$ defined on the interval $[0, L]$, the finite Fourier sine transform $F_s(k)$ is:

$$F_s(k) = \int_0^L f(x) sin\left(\frac{k\pi x}{L}\right) dx, \tag{2.5}$$

where k is a positive integer (mode number) and L is the length of the interval.

The function $f(x)$ can be reconstructed using the inverse finite Fourier sine transform

$$f(x) = \sum_{k=1}^{\infty} F_s(k) sin(\frac{k\pi x}{L}). \tag{2.6}$$

CHAPTER 3

General Solutions for Hydromagnetic Flow of Viscous Fluids between Horizontal Parallel Plates through Porous Medium [21]

3.1 Introduction

In this chapter, the detailed review of research work done by C. Fetecau *et al* [21] is presented. The hydromagnetic flow of an incompressible viscous fluid between two infinitely parallel horizontal plates is analyzed mathematically and analytical solutions are obtained, by taking into account the effects of a porous media. The bottom plate moves with arbitrary velocity. The work highlights the combined impact of magnetic and porous effects on flow behavior by examining a number of theoretically significant motions. Shear stress fields and dimensionless velocity are analyzed in relation to the Reynolds number for motions caused by a plate that is suddenly relocated or accelerates continuously. Moreover, the solutions for couette flow and accelerated flows are established graphically.

3.2 Problem Geometry

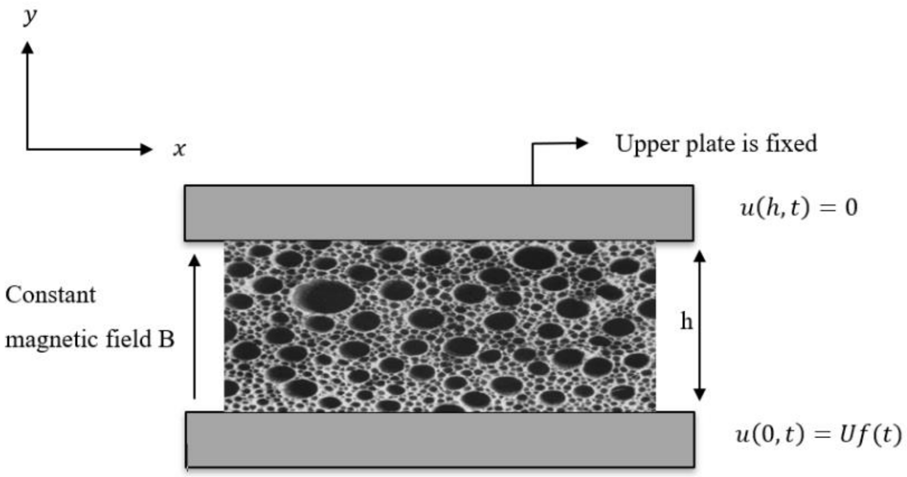

Figure 3.1: Physical sketch of the problem

3.3 Mathematical Formulation

In a porous media, between two infinite horizontal parallel plates spaced h apart, an electrically connected incompressible viscous fluid flows. Plates are subject to a constant magnetic field of intensity B acting perpendicularly. It is possible to disregard the induced magnetic field. At least for partially charged fluids or magnetic liquids with a sufficiently low magnetic Reynolds number, such an assumption is true.

Consider the following flow velocity;

$$\boldsymbol{V} = (u(y,t), 0, 0), \tag{3.1}$$

and the unsteady flows' constitutive equations are provided by

Continuity Equation

$$\boldsymbol{\nabla}.\boldsymbol{V} = 0\ . \tag{3.2}$$

Momentum Equation

$$\rho\,\frac{dV}{dt} = div\,\boldsymbol{T} + \boldsymbol{F}_b + \boldsymbol{R}\,, \tag{3.3}$$

where the Maxwell fluid's stress tensor is provided below

$$\boldsymbol{T} = -p\,\boldsymbol{I} + \mu\boldsymbol{A_1}\,, \tag{3.4}$$

where $\boldsymbol{T}$ is Cauchy stress tensor, $\boldsymbol{F}_b$ is the Lorentz force, μ is the dynamic viscosity, ρ is the density, $\boldsymbol{V}$ is velocity of fluid, p is pressure, d/dt is material time derivative, $\boldsymbol{R}$ is the Darcy resistant, $\intercal$ denotes the transpose and $\boldsymbol{A_1}$ is the first Rivlin-Ericksen tensor provided by

$$\boldsymbol{A_1} = (\boldsymbol{L} + \boldsymbol{L}^{\intercal})\,, \tag{3.5}$$

through

$$\boldsymbol{L} = (grad\boldsymbol{V}) = \begin{bmatrix} 0 & \frac{\partial u}{\partial y} & 0 \\ 0 & 0 & 0 \\ 0 & 0 & 0 \end{bmatrix} \quad \text{and} \quad \boldsymbol{L}^{\intercal} = (grad\boldsymbol{V})^{\intercal} = \begin{bmatrix} 0 & 0 & 0 \\ \frac{\partial u}{\partial y} & 0 & 0 \\ 0 & 0 & 0 \end{bmatrix}.$$

Using Eq. (3.1), we have

$$\boldsymbol{A_1} = \begin{bmatrix} 0 & \frac{\partial u}{\partial y} & 0 \\ \frac{\partial u}{\partial y} & 0 & 0 \\ 0 & 0 & 0 \end{bmatrix}. \tag{3.6}$$

Substituting Eq. (3.6) in Eqs. (3.3) and (3.4) and simplify, we get

$$\tau(y,t) = \mu\,\frac{\partial u(y,t)}{\partial y}\,, \tag{3.7}$$

and

$$\rho \frac{\partial u(y,t)}{\partial t} = \frac{\partial \tau(y,t)}{\partial y} - \sigma B^2 u(y,t) - \frac{\mu}{k} u(y,t) \,, \qquad (3.8)$$

where $\tau(y,t)$ is non-zero shear stress, σ is electrical conductivity of the fluid and k is porous medium's permeability.

Initial and Boundary Conditions

The appropriate boundary and initial condations are described below;

I.C: $$u(y,0) = 0, \qquad 0 \leq y \leq h \,, \qquad (3.9)$$

and

B.C: $$u(0,t) = Uf(t), \quad u(h,t) = 0, \quad t \geq 0 \,, \qquad (3.10)$$

where

i. $f(t) = H(t)$, (Simple Couette Flow)

ii. $f(t) = H(t)t^{a}$, $(a > 0)$, (Flow Induced by an Accelerating Plate)

Consider the form's dimensionless parameters:

$$y^* = \frac{y}{h} \,, \quad t^* = \frac{U}{h} t \,, \quad u^* = \frac{u}{U} \,, \quad \tau^* = \frac{1}{\rho U^2} \tau. \qquad (3.11)$$

In Eqs. (3.8) - (3.10) the following dimensionless problems after eliminate the star notation, we get

$$\tau(y,t) = \frac{1}{Re} \frac{\partial u(y,t)}{\partial y} \,, \qquad (3.12)$$

and

$$\frac{\partial u(y,t)}{\partial t} = \frac{\partial \tau(y,t)}{\partial y} - K_{\text{eff}}\, u(y,t) \qquad 0 < y < h, \quad t > 0 \,. \tag{3.13}$$

I.C $\qquad u(y,0) = 0, \qquad 0 \le y \le 1 \,,$ (3.14)

B.C $\qquad u(0,t) = f(t)\,, \qquad u(1,t) = 0\,, \qquad t \ge 0\,,$ (3.15)

Eliminating $\tau(y,t)$ from Eq. (3.13) produces the following governing equation of the form

$$\frac{\partial u(y,t)}{\partial t} = \frac{1}{Re}\frac{\partial^2 u(y,t)}{\partial y^2} - K_{\text{eff}}\, u(y,t), \qquad 0 < y < 1, \quad t > 0\,, \tag{3.16}$$

where $Re = \frac{Uh}{\nu}$ and $K_{\text{eff}} = M + \frac{1}{K}$ are the effective permeability and Reynolds number.

$$M = \frac{\sigma B^2 h}{\rho U} = \frac{\sigma B^2}{\mu}\frac{h^2}{Re} \quad \text{and} \quad K = \frac{kU}{\upsilon h} = \frac{kRe}{h^2}\,. \tag{3.17}$$

3.4 Solution of the Problem

To solve the dimensionless boundary and initial value problem given by Eqs. (3.14)-(3.16), using the finite fourier sine transform and its inverse,

$$u_{Fs}(n,t) = \int_0^1 u(y,t) Sin(\lambda_n y)dy\,,$$

and

$$u(y,t) = 2\sum_{n=1}^{\infty} u_{Fs}(n,t) Sin(\lambda_n y)\,, \tag{3.18}$$

where $\lambda_n = \; n\pi$.

Therefore, the acquired solution is

$$u(y,t) = \frac{2}{Re}\sum_{n=1}^{\infty}\lambda_n Sin(\lambda_n y)\int_0^t f(t-s)e^{-(\frac{\lambda_n^2}{Re}+K_{\text{eff}})s}ds\ , \tag{3.19}$$

or equivalently,

$$u(y,t) = 2f(t)\sum_{n=1}^{\infty}\frac{\lambda_n Sin(\lambda_n y)}{\lambda_n^2+K_{\text{eff}}Re} - 2\sum_{n=1}^{\infty}\frac{\lambda_n Sin(\lambda_n y)}{\lambda_n^2+K_{\text{eff}}Re} \tag{3.20}$$

$$-\int_0^t f(t-s)e^{-\left(\frac{\lambda_n^2}{Re}+K_{\text{eff}}\right)s}ds\ .$$

The boundary condition Eq. (3.15) in the first part of the Eq. (3.19) and (3.20) appears to be unfulfilled, therefore

$$u(y,t) = (1-y)f(t) - 2K_{\text{eff}}Ref(t)\sum_{n=1}^{\infty}\frac{Sin(\lambda_n y)}{\lambda_n(\lambda_n^2+K_{\text{eff}}Re)} \tag{3.21}$$

$$-2\sum_{n=1}^{\infty}\frac{\lambda_n Sin(\lambda_n y)}{\lambda_n^2+K_{\text{eff}}Re}\int_0^t f'(t-s)e^{-\left(\frac{\lambda_n^2}{Re}+K_{\text{eff}}\right)s}ds\ ,$$

and

$$\tau(y,t) = -\frac{f(t)}{Re} - 2K_{\text{eff}}f(t)\sum_{n=1}^{\infty}\frac{Cos(\lambda_n y)}{\lambda_n^2+K_{\text{eff}}Re} \tag{3.22}$$

$$-\frac{2}{Re}\sum_{n=1}^{\infty}\frac{\lambda_n^2 Cos(\lambda_n y)}{\lambda_n^2+K_{\text{eff}}Re}\int_0^t f'(t-s)e^{-\left(\frac{\lambda_n^2}{Re}+K_{\text{eff}}\right)s}ds\ ,$$

hence, all the boundary condations are satisfied.

The fluid's drag, or nondimensional frictional forces per unit area, acting on two plates is determined by

$$\tau_0(y,t) = \tau(0,t) = -\frac{f(t)}{Re} - 2K_{\text{eff}}f(t)\sum_{n=1}^{\infty}\frac{1}{\lambda_n^2+K_{\text{eff}}Re} \tag{3.23}$$

$$-\frac{2}{Re}\sum_{n=1}^{\infty}\frac{\lambda_n^2}{\lambda_n^2+K_{\text{eff}}Re}\int_0^t f'(t-s)e^{-\left(\frac{\lambda_n^2}{Re}+K_{\text{eff}}\right)s}ds\ ,$$

and

$$\tau_1(y,t) = \tau(1,t) = -\frac{f(t)}{Re} - 2K_{\text{eff}} f(t) \sum_{n=1}^{\infty} \frac{(-1)^n}{\lambda_n^2 + K_{\text{eff}} Re} \tag{3.24}$$
$$-\frac{2}{Re} \sum_{n=1}^{\infty} \frac{(-1)^n \lambda_n^2}{\lambda_n^2 + K_{\text{eff}} Re} \int_0^t f'(t-s) e^{-\left(\frac{\lambda_n^2}{Re} + K_{\text{eff}}\right)s} ds \, .$$

Volume Flux

The formulae for the volume flux $Q(t)$ per unit width of a plane perpendicular to the flow is using Eq. (3.21) in the form

$$Q(t) = \int_0^1 u(y,t) dt = \frac{f(t)}{2} - 4K_{\text{eff}} Re f(t) \sum_{n=1}^{\infty} \frac{1}{\lambda_{2n+1}^2 (\lambda_{2n+1}^2 + K_{\text{eff}} Re)} \tag{3.25}$$
$$-4 \sum_{n=1}^{\infty} \frac{1}{\lambda_{2n+1}^2 + K_{\text{eff}} Re} \int_0^t f'(t-s) e^{-\left(\frac{\lambda_{2n+1}^2}{Re} + K_{\text{eff}}\right)s} ds \, .$$

3.5 Special Cases:

3.5.1 Case I: $f(t) = H(t)$ (Simple Couette Flow)

By replacing $f(t)$ in Eqs. (3.21) and (3.22) with the Heaviside unit step function $H(t)$ and utilizing the knowledge that $H'(t) = \delta(t)$ (the Dirac delta function) and

$$\int_0^t \delta(t-s) h(s) ds = h(t) \, . \tag{3.26}$$

The initial solutions are as follows

$$u_c(y,t) = 1 - y - 2K_{\text{eff}} Re \sum_{n=1}^{\infty} \frac{Sin(\lambda_n y)}{\lambda_n (\lambda_n^2 + K_{\text{eff}} Re)} \tag{3.27}$$
$$-2 \sum_{n=1}^{\infty} \frac{\lambda_n Sin(\lambda_n y)}{\lambda_n^2 + K_{\text{eff}} Re} e^{-\left(\frac{\lambda_n^2}{Re} + K_{\text{eff}}\right)t} ,$$

and

$$\tau_c(y,t) = -\frac{1}{Re} - 2K_{\text{eff}}\sum_{n=1}^{\infty}\frac{Cos(\lambda_n y)}{\lambda_n^2 + K_{\text{eff}}Re} \quad (3.28)$$

$$-\frac{2}{Re}\sum_{n=1}^{\infty}\frac{\lambda_n^2 Cos(\lambda_n y)}{\lambda_n^2 + K_{\text{eff}}Re} e^{-\left(\frac{\lambda_n^2}{Re}+K_{\text{eff}}\right)t} .$$

In a porous material, this is equivalent to hydromagnetic simple Couette flow. A moving plate's frictional force can be shown on

$$\tau_{0c}(t) = -\frac{1}{Re} - 2K_{\text{eff}}\sum_{n=1}^{\infty}\frac{1}{\lambda_n^2 + K_{\text{eff}}Re} \quad (3.29)$$

$$-\frac{2}{Re}\sum_{n=1}^{\infty}\frac{\lambda_n^2}{\lambda_n^2 + K_{\text{eff}}Re} e^{-\left(\frac{\lambda_n^2}{Re}+K_{\text{eff}}\right)t} .$$

Also, the volume flow then becomes

$$Q_c(t) = \frac{1}{2} - 4K_{\text{eff}}Re\sum_{n=1}^{\infty}\frac{1}{\lambda_{2n+1}^2(\lambda_{2n+1}^2 + K_{\text{eff}}Re)} \quad (3.30)$$

$$-4\sum_{n=1}^{\infty}\frac{1}{\lambda_{2n+1}^2 + K_{\text{eff}}Re} e^{-\left(\frac{\lambda_{2n+1}^2}{Re}+K_{\text{eff}}\right)t}, \qquad t > 0 .$$

For $t = 0$, both the volume flux $Q_c(t)$ and the fluid velocity $u_c(y,t)$ are zero, as predicted. When transient components of initial solutions are small, the fluid flows according to steady (permanent) solutions at large time t

$$u_{cp}(y,t) = 1 - y - 2K_{\text{eff}}Re\sum_{n=1}^{\infty}\frac{Sin(\lambda_n y)}{\lambda_n(\lambda_n^2 + K_{\text{eff}}Re)} , \quad (3.31)$$

and

$$\tau_{cp}(y,t) = \frac{1}{Re} - 2K_{\text{eff}}Re\sum_{n=1}^{\infty}\frac{Cos(\lambda_n y)}{\lambda_n^2 + K_{\text{eff}}Re} . \quad (3.32)$$

These solutions meet the boundary requirements and governing equations, but are not affected by the starting condition Eq. (3.14). The frictional force $\tau_{0c}(t)$ on the moving plate and volume flux $Q_c(t)$tend to be stable expressions.

$$\tau_{0cp}(y,t) = -\frac{1}{Re} - 2K_{\text{eff}}\sum_{n=1}^{\infty}\frac{1}{\lambda_n^2+K_{\text{eff}}Re} \ , \tag{3.33}$$

and

$$Q_{cp}(y,t) = \frac{1}{2} - 4K_{\text{eff}}Re\sum_{n=1}^{\infty}\frac{1}{\lambda_{2n+1}^2(\lambda_{2n+1}^2+K_{\text{eff}}Re)} \, , \tag{3.34}$$

for $t \to \infty$.

Direct calculations indicate that the stable solutions from Eqs. (3.31) to (3.34) can be stated in simpler forms. The stable sections $\tau_{cp}(y)$ and $u_{cp}(y)$ from Eq. (3.30) for example, can be expressed in the appropriate forms

$$u_{cp}(y) = \frac{Sinh\left[(1-y)\sqrt{K_{\text{eff}}Re}\right]}{Sinh\sqrt{K_{\text{eff}}Re}} \, , \tag{3.35}$$

and

$$\tau_{cp}(y) = -\sqrt{\frac{K_{\text{eff}}}{Re}}\,\frac{Cosh\left[(1-y)\sqrt{K_{\text{eff}}Re}\right]}{Sinh\sqrt{K_{\text{eff}}Re}} \, . \tag{3.36}$$

Solving the associated boundary value problem yields the analogous expression in the first part of the Eq. (3.35)and (3.36) for the steady component of velocity, $u_{cp}(y)$.

$$\frac{1}{Re}\frac{d^2u(y)}{dy^2} - K_{\text{eff}}u(y) = 0 \, , \qquad u(0) = 1, \quad u(1) = 0 \, . \tag{3.37}$$

The solutions for simple Couette flow and hydromagnetic simple Couette flow through porous media are simple to obtain, with $K \to \infty$ and $M \to 0,$ respectively, and $K_{\text{eff}} = 0$. Velocity expression for basic Couette flow

$$u(y,t) = 1 - y - 2\sum_{n=1}^{\infty} \frac{Sin(\lambda_n y)}{\lambda_n} e^{(-\frac{\lambda_n^2}{Re}t)} . \tag{3.38}$$

3.5.2 Case II: $f(t) = H(t)t^a$ $(a > 0)$ (Flow Induced by an Accelerating Plate)

Changing $f(t)$ in Eqs. (3.21) and (3.22) to $H(t)t^a$ $(a > 0)$ yields solutions for fluid motion caused by an accelerated plate.

$$u_1(y,t) = (1-y)t - 2K_{\text{eff}}Ret\sum_{n=1}^{\infty} \frac{Sin(\lambda_n y)}{\lambda_n(\lambda_n^2 + K_{\text{eff}}Re)} \tag{3.39}$$

$$-2Re\sum_{n=1}^{\infty} \frac{\lambda_n Sin(\lambda_n y)}{(\lambda_n^2 + K_{\text{eff}}Re)^2}\{1 - e^{-\left(\frac{\lambda_n^2}{Re}+K_{\text{eff}}\right)t}\} ,$$

and

$$\tau_1(y,t) = \frac{t}{Re} - 2K_{\text{eff}}t\sum_{n=1}^{\infty} \frac{Cos(\lambda_n y)}{\lambda_n^2 + K_{\text{eff}}Re} \tag{3.40}$$

$$-2\sum_{n=1}^{\infty} \frac{\lambda_n^2 Cos(\lambda_n y)}{(\lambda_n^2 + K_{\text{eff}}Re)^2}\{1 - e^{-\left(\frac{\lambda_n^2}{Re}+K_{\text{eff}}\right)t}\} ,$$

equivalent to $f(t) = H(t)$ when the bottom plate is continuously accelerated. Eqs. (3.23 - 3.25) can be used to calculate frictional forces and volume flow between two plates. Furthermore, considering the formulations of $u_{cp}(y)$ and $\tau_{cp}(y)$ provided by Eqs. (3.27) and (3.28) it is easy to establish that

$$u_n(y,t) = (n!)\int_0^t \int_0^{s_1} \int_0^{s_2}, \dots, \int_0^{s_{n-1}} u_c(y,s_n)ds_1 ds_2, \dots, ds_n , \tag{3.41}$$

$$\tau_n(y,t) = (n!)\int_0^t \int_0^{s_1} \int_0^{s_2}, \dots, \int_0^{s_{n-1}} \tau_c(y,s_n)ds_1 ds_2, \dots, ds_n , \tag{3.42}$$

where $u_n(y,t)$ and $\tau_n(y,t)$ are solutions corresponding to $f(t) = H(t)t^n$. Knowing the solutions $u_c(y,t)$ and $\tau_c(y,t)$ of the basic Couette flow allows for determining the solutions $u_n(y,t)$ and $\tau_n(y,t)$ by simple or multiple integrations.

3.6 Results and Discussion

Analytical study of the hydromagnetic flow of viscous fluids between parallel plates immersed in a porous material was conducted. General formulae in series and integral form have been found for the nonvoid shear stress fields and velocity, as well as for the volume flux $Q(t)$ per unit width. Moreover, motion characteristics rely on the porous and magnetic parameters K and M via the effective permeability. The impact of Reynolds number, and the combined porous and magnetic effect on velocity field and shear stress are graphically undefined and depicted in Figs. 3.2-3.7.

Fig. 3.2 shows the comparison between two forms of steady components of velocities given by Eqs. (3.32) and (3.36) and comparison of steady components of shear stress is given by Eqs. (3.33) and (3.37) for different value of K_{eff}, respectively. It can be seen that by increasing the value of effective permeability K_{eff} the velocity profile is decreasing. Moreover, combined effect of porosity and constant magnetism shows the retardation in fluid motion, for two different forms of the velocity profile and the corresponding shear stress.

Figs. 3.3-3.5 and 3.6-3.8 show the fluctuation of shear stress and velocity fields versus y for flows caused by uniform or constantly accelerating motion of the bottom plate for different values of Reynolds number (Re), effective permeability (K_{eff}), and time (t). In both cases, the fluid shear stress $\tau\ (y,t)$ and velocity $u\ (y,t)$ in terms of absolute value gradually decline from maximum values on the moving plate to zero values on the stationary plate. The fluid velocity as a result of these figures increases with time and drops for increased Reynolds numbers Re or K_{eff} over the whole flow domain.

Figs. 3.5 and 3.8 cannot accurately forecast the influence of a magnetic field or a porous media on velocity and shear stress due to the unlimited range of M and K values. However, these graphical representations apply to the same fluid flow for which $M = 1, 3$ or 7 in the absence of a porous media, or for movements in which the magnetic field is absent, and $K = 1$, $\frac{1}{3}$ or

$\frac{1}{7}$. As a result, the fluid velocity decreases with respect to the magnetic parameter M while increases with respect to K. More precisely, the presence of a magnetic field or the porous material suggests a reduction in the fluid velocity.

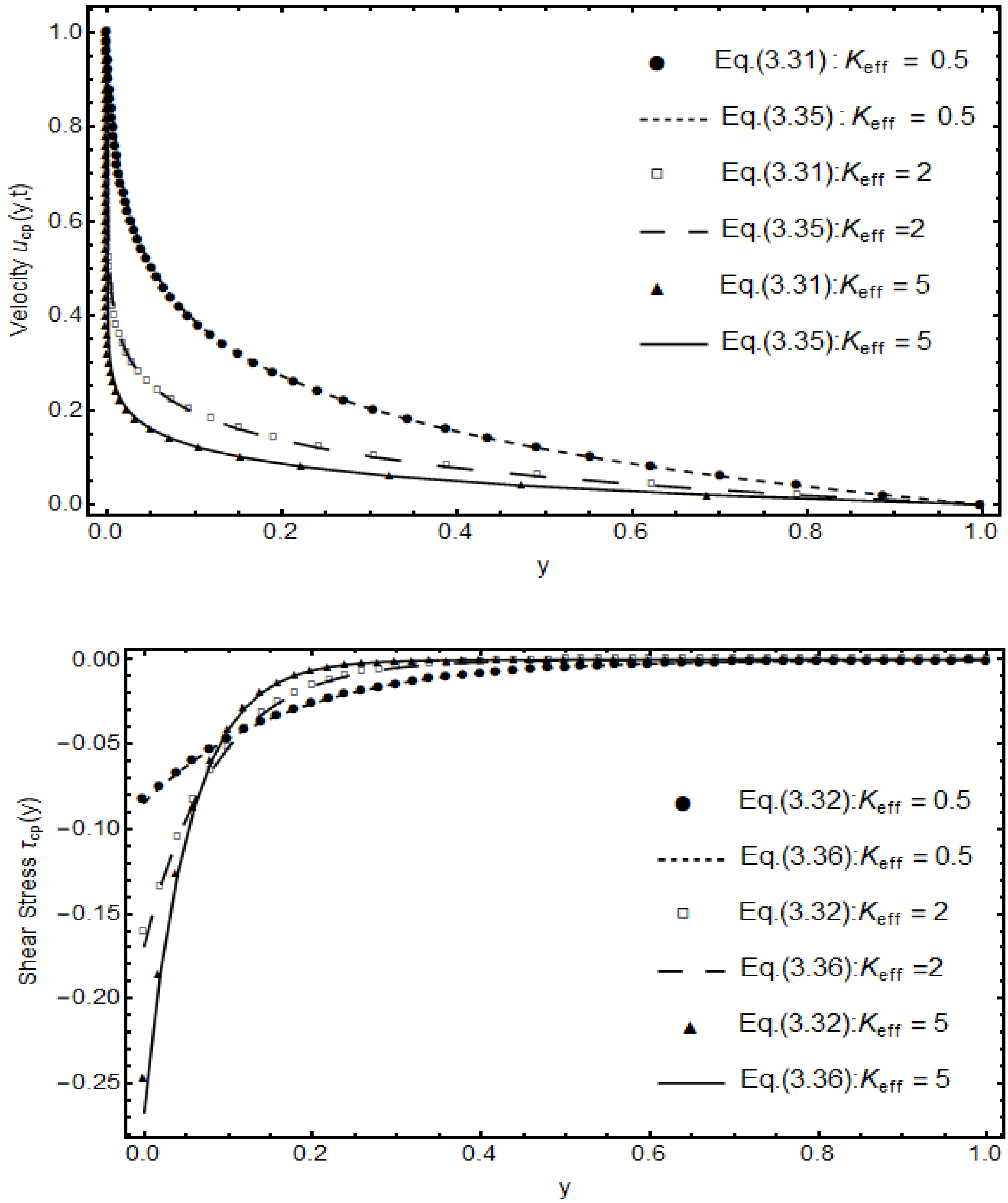

Figure 3.2: Profile of steady components $u_{cp}(y,t)$ and $\tau_{cp}(y,t)$ for different values of K_{eff} and $Re = 70$.

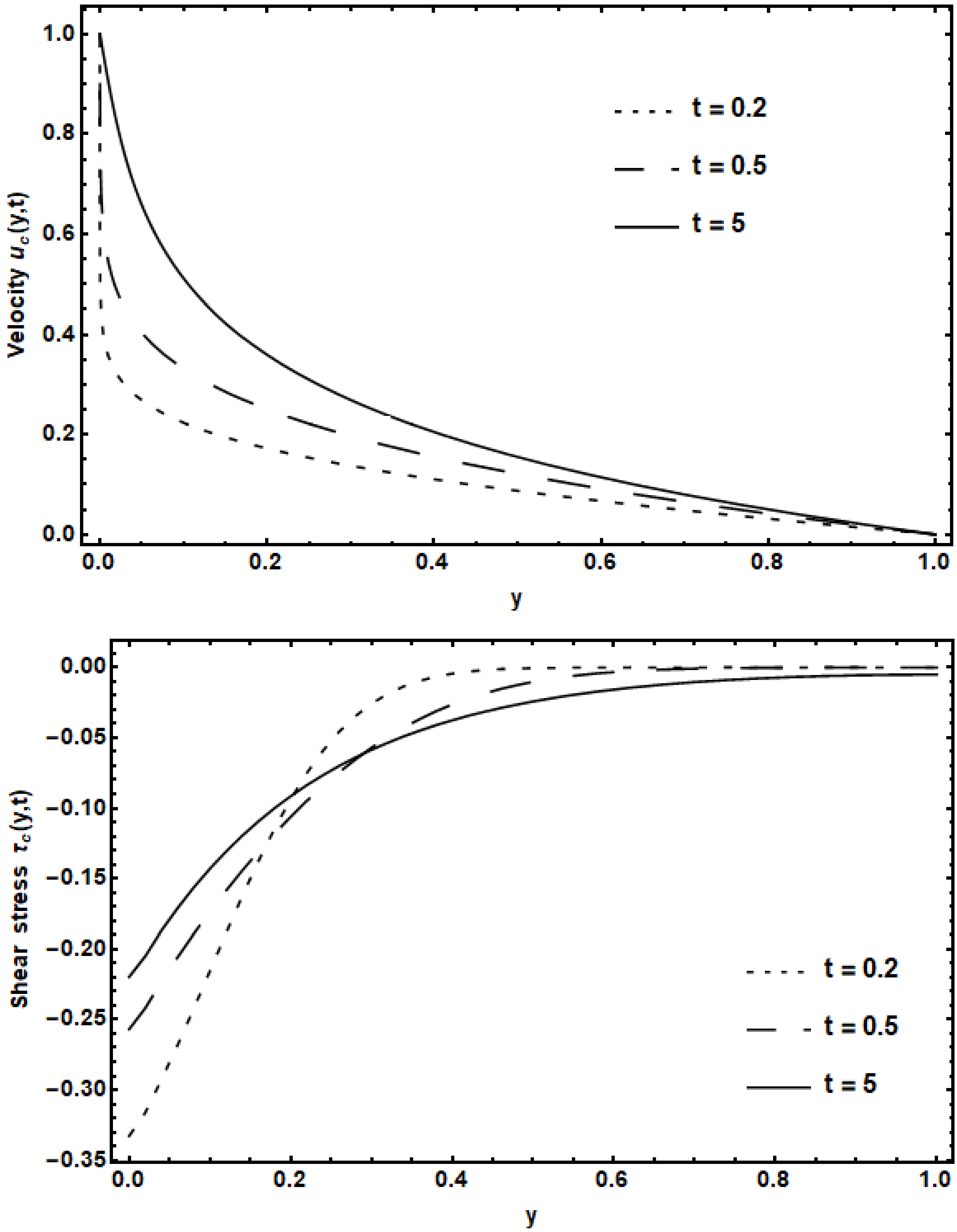

Figure 3.3: Velocity and shear stress variations for t provided by Eqs. (3.27) and (3.28).

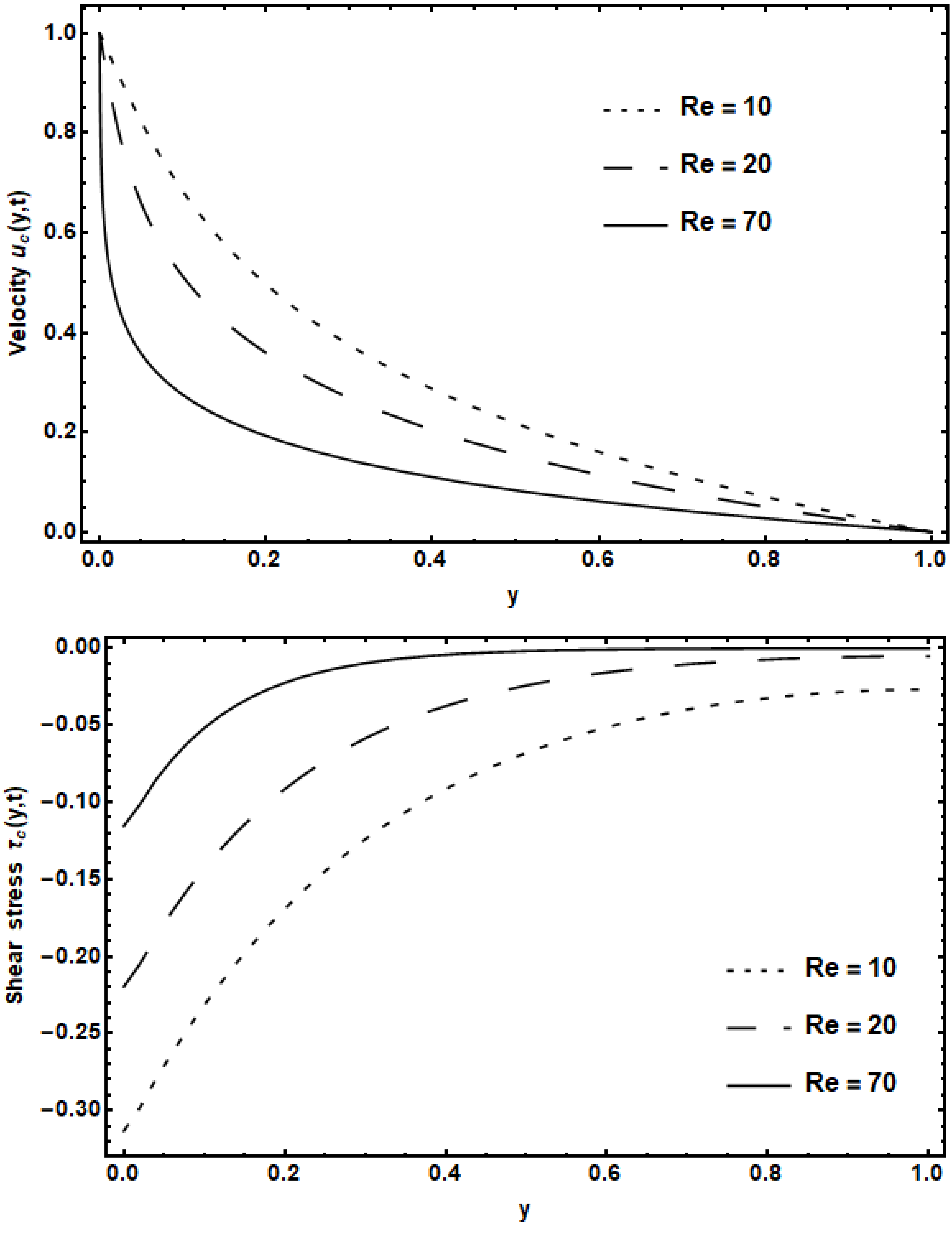

Figure 3.4: Velocity and shear stress variations for Re provided by Eqs. (3.27) and (3.28).

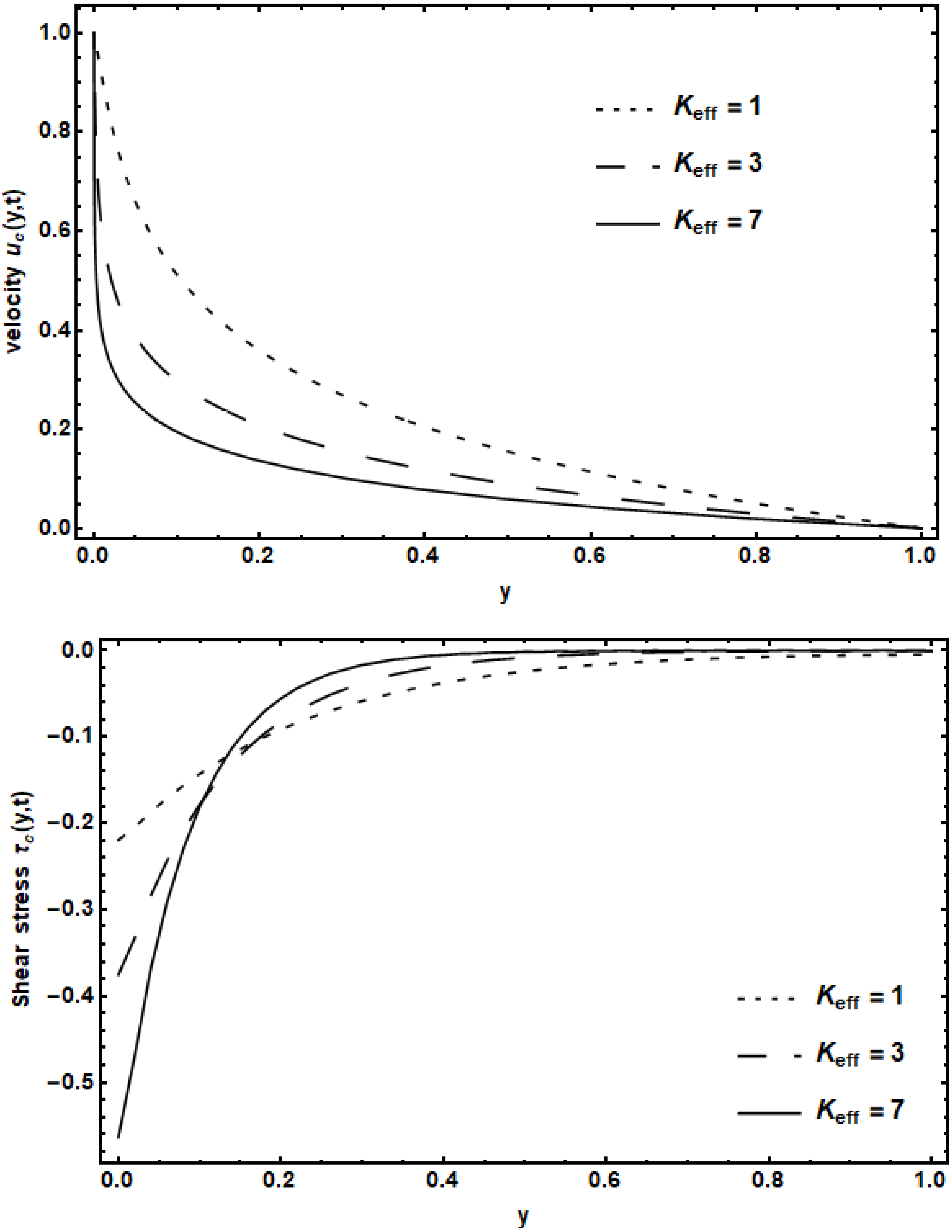

Figure 3.5: Velocity and shear stress variations for K_{eff} provided by Eqs. (3.27) and (3.28).

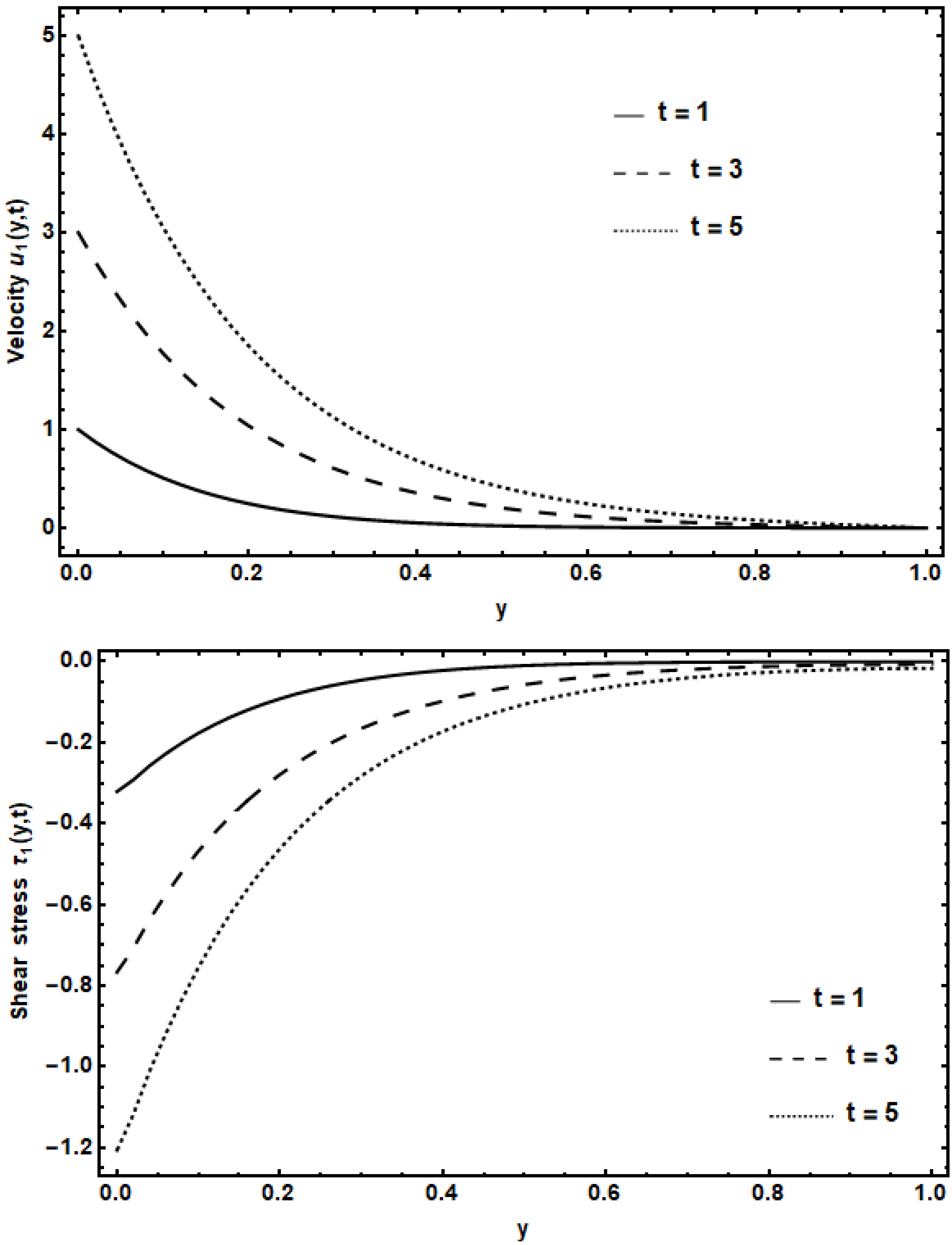

Figure 3.6: Velocity and shear stress variations for t provided by Eqs. (3.39) and (3.40).

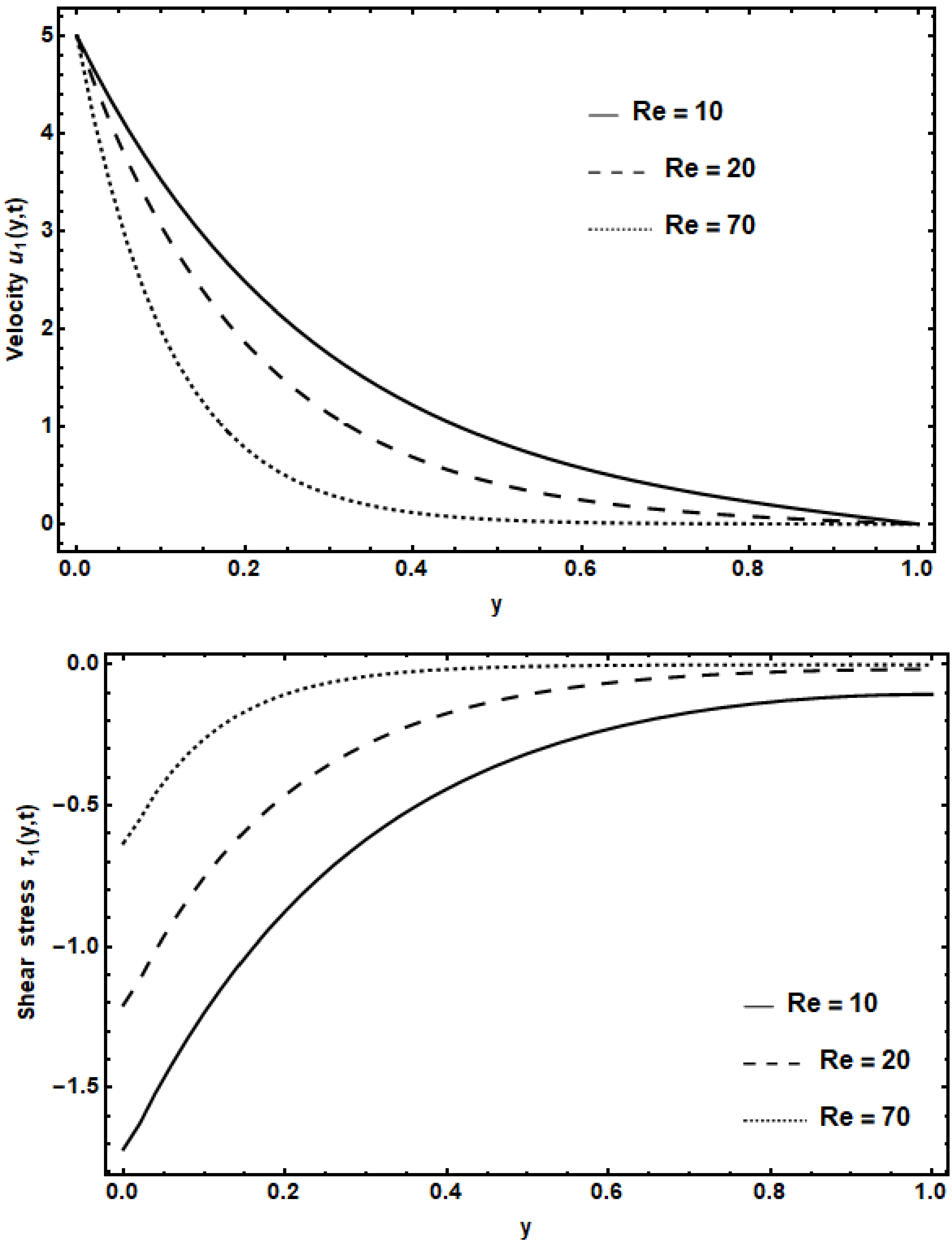

Figure 3.7: Velocity and shear stress variations for Re provided by Eqs. (3.39) and (3.40).

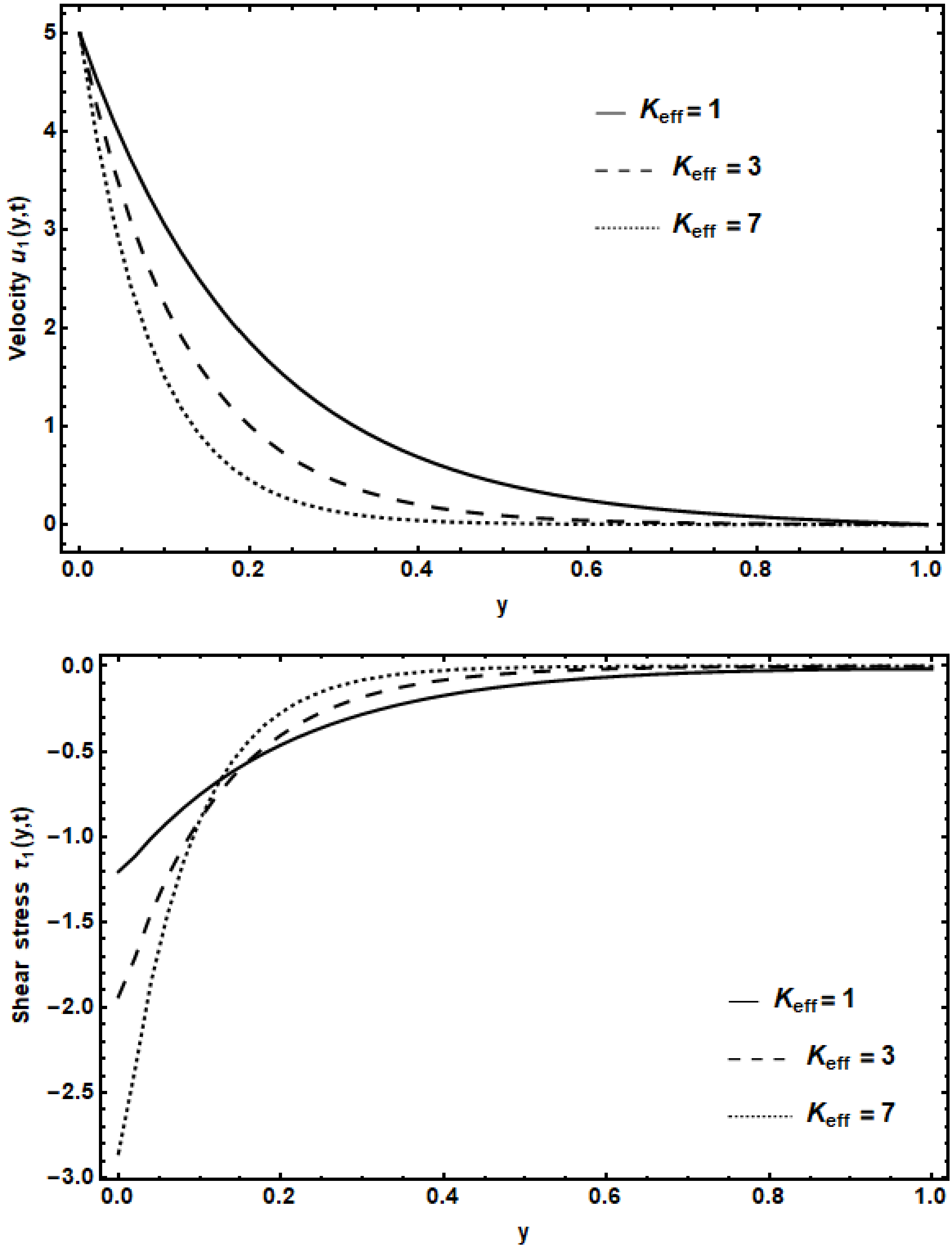

Figure 3.8: Velocity and shear stress variations for K_{eff} provided by Equ. (3.39) and (3.40)

CHAPTER 4

General Solutions for Magnetohydrodynamics Flow of a Viscoelastic Fluid through Porous Medium

4.1 Introduction

Consider unsteady, one dimensional and incompressible hydromagnetic Maxwell fluid that are along the x-axis between two parallel, horizontal plates. The impact of porosity is considered. The fluid motion is created by one of the plates is couette flow or accelerating in its own plane, and the solutions meet all initial and boundary requirements. FFST is used to find the precise exact analytical solution for the dimensionless velocity field, shear stress, and volume flux. The limiting case for the Newtonian fluid [21] is recovered. Moreover, the effects of various pertinent parameter of the flow are discussed through graphs.

4.2 Mathematical Modeling

One dimensional, unsteady, Incompressible , hydromagnetic Maxwell fluid lies between two infinite horizontal parallel plates at a distance h apart is considered. Also, the effect of porous media are also considered. The velocity and stress field profiles of the form determine the flow,

$$\boldsymbol{V} = (u(y,t), 0, 0) , \quad \text{and} \quad \mathbf{S} = \mathbf{S}(y,t) , \tag{4.1}$$

and constitutive equations for the unsteady flow are given by:

Continuity Equation

$$\boldsymbol{\nabla}.\boldsymbol{V} = 0 , \tag{4.2}$$

Momentum Equation

$$\rho \frac{d\boldsymbol{V}}{dt} = \mathrm{div}\, \boldsymbol{T} + \boldsymbol{F}_b + \boldsymbol{R} , \tag{4.3}$$

where the Maxwell fluid's stress tensor is provided below:

$$\boldsymbol{T} = -p\, \boldsymbol{I} + \boldsymbol{S} , \tag{4.4}$$

and

$$\boldsymbol{S} + \lambda \left(\frac{D\boldsymbol{S}}{Dt}\right) = \mu \boldsymbol{A_1} , \tag{4.5}$$

in which

$$\frac{D\boldsymbol{S}}{Dt} = \frac{d\boldsymbol{S}}{dt} - \boldsymbol{LS} - \boldsymbol{SL}^{\intercal} , \tag{4.6}$$

where $\boldsymbol{T}$ is Cauchy stress tensor, $\boldsymbol{S}$ is extra stress tensor, $\boldsymbol{F}_b$ is the Lorentz force , $\boldsymbol{V}$ is velocity of fluid, p is pressure, $\frac{d}{dt}$ is material time derivative, $\frac{D}{Dt}$ is upper convective time derivative, λ is the relaxation time, $\boldsymbol{L}$ is the velocity gradient, $\mathbf{A_1}$ is the first tensor of Rivlin-Ericksen , ⊺ denotes the transpose, $\boldsymbol{R}$ is the Darcy resistant and μ is the dynamic viscosity is provided by:

$$\boldsymbol{A_1} = (\boldsymbol{L} + \boldsymbol{L}^{\intercal}) \,, \tag{4.7}$$

through

$$\boldsymbol{L} = (\text{grad}\, \boldsymbol{V}) = \begin{bmatrix} 0 & \frac{\partial u}{\partial y} & 0 \\ 0 & 0 & 0 \\ 0 & 0 & 0 \end{bmatrix} \quad \text{and} \quad \boldsymbol{L}^{\intercal} = (\text{grad}\, \boldsymbol{V})^{\intercal} = \begin{bmatrix} 0 & 0 & 0 \\ \frac{\partial u}{\partial y} & 0 & 0 \\ 0 & 0 & 0 \end{bmatrix}.$$

Using Eq. (4.1), we have

$$\boldsymbol{A_1} = \begin{bmatrix} 0 & \frac{\partial u}{\partial y} & 0 \\ \frac{\partial u}{\partial y} & 0 & 0 \\ 0 & 0 & 0 \end{bmatrix}, \tag{4.8}$$

$$\frac{D\boldsymbol{S}}{Dt} = \begin{bmatrix} \frac{\partial}{\partial t} S_{xx} - 2S_{yx}\frac{\partial u}{\partial t} & \frac{\partial}{\partial t} S_{xy} - S_{yy}\frac{\partial u}{\partial t} & \frac{\partial}{\partial t} S_{xz} - S_{yz}\frac{\partial u}{\partial t} \\ \frac{\partial}{\partial t} S_{yx} - S_{yy}\frac{\partial u}{\partial t} & \frac{\partial}{\partial t} S_{yy} & \frac{\partial}{\partial t} S_{yz} \\ \frac{\partial}{\partial t} S_{zx} - S_{zy}\frac{\partial u}{\partial t} & \frac{\partial}{\partial t} S_{zy} & \frac{\partial}{\partial t} S_{zz} \end{bmatrix}. \tag{4.9}$$

Substitution of Eqs. (4.8) and (4.9) into Eq. (4.4) one can write Eq. (4.5) in the component form as

$$S_{xx} + \lambda\left(\frac{\partial S_{xx}}{\partial t} - 2\lambda S_{yx}\frac{\partial u}{\partial y}\right) = 0 \,, \tag{4.10}$$

$$S_{xy} + \lambda\left(\frac{\partial S_{xy}}{\partial t} - S_{yy}\frac{\partial u}{\partial y}\right) = \mu\frac{\partial u}{\partial y} \,, \tag{4.11}$$

$$S_{xz} - \lambda \left(\frac{\partial S_{xz}}{\partial t} - S_{yz} \frac{\partial u}{\partial y} \right) = 0 \,, \tag{4.12}$$

$$S_{yy} + \lambda \left(\frac{\partial S_{yy}}{\partial t} \right) = 0 \,, \tag{4.13}$$

$$S_{yz} + \lambda \left(\frac{\partial S_{yz}}{\partial t} \right) = 0 \,, \tag{4.14}$$

and

$$S_{zz} + \lambda \left(\frac{\partial S_{zz}}{\partial t} \right) = 0 \,. \tag{4.15}$$

Considering initial conditions of the form

$$S(y,0) = \frac{\partial S(y,0)}{\partial t} = 0 \,. \tag{4.16}$$

Eqs. (4.10) - (4.13) becomes

$$S_{xx} = S_{yz} = S_{zz} = S_{xz} = S_{yy} = 0 \,. \tag{4.17}$$

4.3 Statement of the Problem

Consider unsteady, incompressible and hydromagnetic Maxwell fluid placed between two parallel plates along x-axis. Initially, both the plates and the fluid are at rest. At $t = 0^+$, the lower plate starts to move in its own plane with the velocity $Uf(t)$. The fluid moves gradually due to shear and the continuity equation is true for Eq. (4.2). In the constitutive Eqs. (4.11), introduce the velocity field provided by Eq. (4.1), and since:

$$\boldsymbol{V} = (u(y,t), 0, 0), \quad \text{and} \quad \mathbf{S}(y,0) = 0 \,, \; 0 \le y \le h \,. \tag{4.18}$$

therefore, we get the following statement of the form

$$\left(1+\lambda\frac{\partial}{\partial t}\right)S_{xy}(y,t)=\mu\frac{\partial u(y,t)}{\partial y}, \tag{4.19}$$

or

$$\left(1+\lambda\frac{\partial}{\partial t}\right)\tau(y,t)=\mu\frac{\partial u(y,t)}{\partial y}, \tag{4.20}$$

where $\tau(y,t)=S_{xy}(y,t)$ are the non-trivial component of shear stress and

$$\rho\frac{\partial u(y,t)}{\partial t}=-\frac{\partial p}{\partial x}+\frac{\partial\tau(y,t)}{\partial y}+F_x+R_x(y,t), \tag{4.21}$$

$$0=-\frac{\partial p}{\partial y}, \tag{4.22}$$

and

$$0=-\frac{\partial p}{\partial z} \qquad \Rightarrow p\neq p(y,z), \tag{4.23}$$

where ρ is the fluid density, F_x is the body force along the x- axis and $R_x(y,t)$ is the Darcy resistance along x- axis [28]:

$$\left(1+\lambda\frac{\partial}{\partial t}\right)R_x=-\frac{\mu\varphi}{k}u(y,t), \tag{4.24}$$

where φ is the porous medium's permeability and k is the porosity parameter. The equation that results from removing $\tau(y,t)$ from Eqs. (4.20) and (4.21) while keeping in mind Eq. (4.24), looks like:

$$\left(1+\lambda\frac{\partial}{\partial t}\right)\frac{\partial u(y,t)}{\partial t}=\nu\frac{\partial^2 u(y,t)}{\partial y^2}+\frac{1}{\rho}\left(1+\lambda\frac{\partial}{\partial t}\right)\sigma B_o^2\mu-\frac{\nu}{k}u(y,t),$$

$$0<y<h,\ t>0, \tag{4.25}$$

where $\nu=\frac{\mu}{k}$ is the fluid of kinematic viscosity. The appropriate initial and boundary conditions are defined below:

I.C $u(y,0) = 0\,, \qquad \frac{\partial u(y,t)}{\partial t}\big|_{t=0} = 0\,, \qquad 0 \le y \le h\,,$ (4.26)

and

B.C $u(0,t) = f(t)\,, \quad u(h,t) = 0\,, \qquad t > 0\,.$ (4.27)

4.4 Solution of the Problem

To make the recommended model non-dimensional, dimensionless variables are defined:

$$y^* = \frac{y}{h}\,, \quad t^* = \frac{U}{h}t\,, \quad u^* = \frac{u}{U}\,, \quad \tau^* = \frac{1}{\rho U^2}\tau\ . \tag{4.28}$$

Substituting Eq. (4.28) into Eqs. (4.25) – (4.27), the following dimensionless problem is obtained after removing the star notation

$$\left(1 + We\frac{\partial}{\partial t}\right)\frac{\partial u(y,t)}{\partial t} = \frac{1}{Re}\frac{\partial^2 u}{\partial y^2} - K_{\text{eff}}\,u(y,t) - MWe\frac{\partial u(y,t)}{\partial t}\,,\ 0 < y < h, \quad t > 0, \tag{4.29}$$

$$u(y,0) = \frac{\partial u(y,t)}{\partial t}\big|_{t=0} = 0, \quad \text{for} \quad 0 \le y \le 1, \tag{4.30}$$

and

$$u(0,t) = 1, \text{ and } \quad u(1,t) = 0 \quad \text{if} \quad t > 0, \tag{4.31}$$

where in Eq. (4.29), K_{eff} is the effective permeability, We is the Weissenberg number and Re is the Reynolds number defined below,

$$Re = \frac{Uh}{\nu}, \quad We = \frac{\lambda u}{h}, \quad K_{\text{eff}} = M + \frac{1}{K}\ , \quad K = \frac{kU}{\nu h}, \quad M = \frac{\sigma B^2 h}{\rho U}\ . \qquad (4.32)$$

Dimensionless forms of the (4.20) is given below,

$$\left(1 + We\frac{\partial}{\partial t}\right)\tau(y,t) = \frac{1}{Re}\frac{\partial u(y,t)}{\partial y}\ , \qquad (4.33)$$

the corresponding initial condations are:

$$\tau(y,0) = 0, \qquad 0 \le y \le 1. \qquad (4.34)$$

Multiplying Eq. (4.29) by $sin(\lambda_n y)$, where $\lambda_n = n\pi$, and while keeping the condition in mind, the result is integrated with respect to y from 0 to 1 by using Eq. (4.31), it results that,

$$ReWe\frac{\partial^2 u_{Fs}(t)}{\partial t^2} + Re(1 + MWe)\frac{\partial u_{Fs}(t)}{\partial t} + Re\left(K_{\text{eff}} + \frac{\lambda_n^2}{Re}\right)u_{Fs}(t) = \lambda_n f(t)\ ,$$

$$t > 0\ , \qquad (4.35)$$

with initial conditions

$$u_{Fs}(0) = \frac{\partial u_{Fs}}{\partial t}|_{t=0} = 0, \qquad \text{n}= 1,2,3 \ldots \ldots .., \qquad (4.36)$$

where $u_{Fs}(t)$ is the finite Fourier sine transform of $u(y,t)$, and $\lambda_n = n\pi$.

4.4.1 Case I: $f(t) = H(t)$ (Simple Couette Flow)

The solution of the Eq. (4.35) by using initial conditions Eq. (4.36) is given below:

$$u_{Fs}(n,t) = \frac{\lambda_n}{\mu_n^2}\left(\frac{r_{1n}}{r_{2n}-r_{1n}}\right)e^{r_{2n}t} - \frac{\lambda_n}{\mu_n^2}\left(\frac{r_{2n}}{r_{2n}-r_{1n}}\right)e^{r_{1n}t} + \frac{\lambda_n}{\mu_n^2}, \tag{4.37}$$

where $r_{1n}, r_{2n} = \frac{-(1+MWe)\pm\sqrt{(1+MWe)^2-4We\frac{\mu_n^2}{Re}}}{2We}$ are the causes and $\mu_n^2 = \lambda_n^2 + k_{eff}Re$.

Using Eq. (4.37) and the inverse FFST, we obtain:

$$u(y,t) = 2\sum_{n=1}^{\infty}\left\{\left(\frac{r_{1n}}{r_{2n}-r_{1n}}\right)e^{r_{2n}t} - \left(\frac{r_{2n}}{r_{2n}-r_{1n}}\right)e^{r_{1n}t}\right\}\frac{\lambda_n Sin(\lambda_n y)}{\mu_n^2}$$

$$+2\sum_{n=1}^{\infty}\frac{\lambda_n Sin(\lambda_n y)}{\mu_n^2}, \tag{4.38}$$

or equivalently

$$u_c(y,t) = 1 - y - 2K_{\text{eff}}Re\sum_{n=1}^{\infty}\frac{Sin(\lambda_n y)}{\lambda_n(\lambda_n^2+K_{\text{eff}}Re)}$$

$$-2\sum_{n=1}^{\infty}\frac{\lambda_n Sin(\lambda_n y)}{\mu_n^2}\left[\left(\frac{r_{2n}}{r_{2n}-r_{1n}}\right)e^{r_{1n}t} - \left(\frac{r_{1n}}{r_{2n}-r_{1n}}\right)e^{r_{2n}t}\right]. \tag{4.39}$$

Introducing $u(y,t)$ from Eq. (4.39) into Eq. (4.33) and integrating the result by keeping in mind the condition Eq.(4.34), it results that:

$$\tau_c(y,t) = (1 - e^{-\frac{t}{We}})\left(-\frac{1}{Re} - 2K_{\text{eff}}\sum_{n=1}^{\infty}\frac{Cos(\lambda_n y)}{\mu_n^2}\right)$$

$$-\frac{2}{Re}\sum_{n=1}^{\infty}\frac{\lambda_n^2 Cos(\lambda_n y)}{\mu_n^2}\left[\frac{r_{2n}(1+We\,r_{2n})e^{r_{1n}t} - r_{1n}(1+We\,r_{1n})e^{r_{2n}t}}{(r_{2n}-r_{1n})(1+We\,r_{1n})(1+We\,r_{2n})}\right]. \tag{4.40}$$

In a porous material, this is equivalent to hydromagnetic simple Couette flow. For example, frictional force on a moving plate can be

$$\tau_{0c}(t) = (1 - e^{-\frac{t}{We}})(-\frac{1}{Re} - 2K_{\text{eff}} \sum_{n=1}^{\infty} \frac{1}{\mu_n^2})$$

$$- \frac{2}{Re} \sum_{n=1}^{\infty} \frac{\lambda_n^2}{\mu_n^2} \left[\frac{r_{2n}(1+We\, r_{2n}) e^{r_{1n}t} - r_{1n}(1+We\, r_{1n}) e^{r_{2n}t}}{(r_{2n}-r_{1n})(1+We\, r_{1n})(1+We\, r_{2n})} \right]. \qquad (4.41)$$

The volume flux $Q(t)$ per unit width of a plane normal to the flow is also a crucial factor in this scenario. Eq. (4.39) describes its expression

$$Q_c(t) = \int_0^1 u_c(y,t)dy = \frac{1}{2} - 4K_{\text{eff}} Re \sum_{n=1}^{\infty} \frac{1}{\lambda_{2n+1}^2(\lambda_{2n+1}^2 + K_{\text{eff}}\, Re)}$$

$$-4 \sum_{n=1}^{\infty} \frac{1}{\lambda_{2n+1}^2 + K_{\text{eff}}\, Re} \left[\left(\frac{r_{2n}}{r_{1n}-r_{2n}} \right) e^{r_{1n}t} - \left(\frac{r_{1n}}{r_{1n}-r_{2n}} \right) e^{r_{2n}t} \right], \; t > 0 \,. \qquad (4.42)$$

For $t = 0$, both the volume flux $Q_c(t)$ and the fluid velocity $u_c(y,t)$ are zero, as predicted. When transient components of initial solutions are small, the fluid flows according to steady (permanent) solutions at large time t.

$$u_{cp}(y,t) = 1 - y - 2K_{\text{eff}} Re \sum_{n=1}^{\infty} \frac{Sin(\lambda_n y)}{\lambda_n(\lambda_n^2 + K_{\text{eff}} Re)} \;, \qquad (4.43)$$

and

$$\tau_{cp}(y,t) = \frac{1}{Re} - 2K_{\text{eff}} Re \sum_{n=1}^{\infty} \frac{Cos(\lambda_n y)}{\lambda_n^2 + K_{\text{eff}} Re} \;. \qquad (4.44)$$

These solutions meet the boundary requirements and governing equations, but are not affected by the initial condition (Eq. 4.26). The frictional force $\tau_{0c}(t)$ on the moving plate and volume flux $Q_c(t)$ tend to be stable expression.

$$\tau_{0cp}(y,t) = -\frac{1}{Re} - 2K_{\text{eff}} \sum_{n=1}^{\infty} \frac{1}{\lambda_n^2 + K_{\text{eff}} Re} \;, \qquad (4.45)$$

and

$$Q_{cp}(y,t) = \frac{1}{2} - 4K_{\text{eff}}Re\sum_{n=1}^{\infty} \frac{1}{\lambda_{2n+1}^2(\lambda_{2n+1}^2 + K_{\text{eff}}Re)} \quad , \tag{4.46}$$

for $t \to \infty$.

Direct calculations indicate that the stable solutions from Eqs. (4.43) - (4.46) can be stated in simpler forms. The stable sections $\tau_{cp}(y)$ and $u_{cp}(y)$ from Eqs. (4.43) and (4.44), for example, can be expressed in the appropriate forms defined blow

$$u_{cp}(y) = \frac{Sinh\left[(1-y)\sqrt{K_{\text{eff}}Re}\right]}{Sinh\sqrt{K_{\text{eff}}Re}}, \tag{4.47}$$

and

$$\tau_{cp}(y) = -\sqrt{\frac{K_{\text{eff}}}{Re}}\frac{Cosh\left[(1-y)\sqrt{K_{\text{eff}}Re}\right]}{Sinh\sqrt{K_{\text{eff}}Re}}. \tag{4.48}$$

Solving the associated boundary value problem yields the analogous expression in the first part of the Eq. (4.45) for the steady component of velocity $u_{cp}(y)$.

4.4.2 Case II: $f(t) = H(t)t^a (a > 0)$ (Flow Induced by an Accelerate Plate)

The solution of the Eq. (4.35) by using initial conditions Eq. (4.36) is given below:

$$u_{Fs}(n,t) = \left(\frac{\mu_n^2 + r_{1n}Re(1+M\,We)}{r_{2n} - r_{1n}}\right)e^{r_{2n}t} - \left(\frac{\mu_n^2 + r_{2n}Re(1+M\,We)}{r_{2n} - r_{1n}}\right)e^{r_{1n}t} + \frac{\lambda_n}{\mu_n^2}\left(t - \frac{Re}{\mu_n^2}\right), \tag{4.49}$$

where $r_{1n}, r_{2n} = \frac{-(1+MWe) \pm \sqrt{(1+MWe)^2 - 4We\frac{\mu_n^2}{Re}}}{2We}$ are the roots and $\mu_n^2 = \lambda_n^2 + k_{\text{eff}}\text{Re}$.

Using Eq. (4.49) and the inverse FFST, we obtain:

$$u_1(y,t) = \sum_{n=1}^{\infty}\left\{t - \frac{Re}{\mu_n^2} - \frac{(\mu_n^2 + r_{1n}Re(1+M\,We))e^{r_{2n}t} + (\mu_n^2 + r_{2n}Re(1+M\,We)e^{r_{1n}t}}{(r_{2n}-r_{1n})\mu_n^4}\right\}$$

$$\times \frac{\lambda_n Sin(\lambda_n y)}{\mu_n^2}, \qquad (4.50)$$

or equivalently

$$u_1(y,t) = (1-y)t - 2tK_{\text{eff}}Re\sum_{n=1}^{\infty}\frac{Sin(\lambda_n y)}{\lambda_n\mu_n^2} - 2Re\sum_{n=1}^{\infty}[1$$

$$+ \frac{(\mu_n^2 + r_{1n}Re(1+M\,We))e^{r_{2n}t} - (\mu_n^2 + r_{2n}Re(1+M\,We))e^{r_{1n}t}}{Re(r_{2n}-r_{1n})}]\frac{\lambda_n Sin(\lambda_n y)}{\mu_n^4}. \qquad (4.51)$$

Introducing $u(y,t)$ from Eq. (4.51) into Eq. (4.33) and integrating the result by keeping in mind the initial condition Eq.(4.34), it results that:

$$\tau_1(y,t) = -\frac{t}{Re} + \frac{We}{Re}(1 - e^{-\frac{t}{We}}) - 2K_{\text{eff}}\sum_{n=1}^{\infty}\{t - (We - \frac{\lambda_n^2}{\mu_n^2}(1 + M\,We)$$

$$\times (1 - e^{-\frac{t}{We}}))\}\frac{Cos(\lambda_n y)}{\mu_n^2} - \frac{2}{Re}\sum_{n=1}^{\infty}\{\frac{\mu_n^2 + r_{1n}Re(1+M\,We)}{1+We\,r_{2n}}e^{r_{1n}t}$$

$$-\left(\frac{\mu_n^2 + r_{2n}Re(1+M\,We)}{1+We\,r_{1n}}\right)e^{r_{1n}t}\}\frac{\lambda_n^2 Cos(\lambda_n y)}{\mu_n^4(r_{2n}-r_{1n})} + \frac{2}{Re}e^{-\frac{t}{We}}$$

$$\times\sum_{n=1}^{\infty}\left\{\frac{((\mu_n^2 + r_{1n}Re(1+M\,We))(1+We\,r_{1n})) - (\mu_n^2 + r_{2n}Re(1+M\,We)(1+We\,r_{2n})}{(1+We\,r_{1n})(1+We\,r_{2n})(r_{2n}-r_{1n})}\right\}$$

$$\times\frac{\lambda_n^2 Cos(\lambda_n y)}{\mu_n^4}. \qquad (4.52)$$

4.5 limiting Case ($We \to 0$, Newtonian fluid)

Taking $We \to 0$ into Eqs. (4.39), (4.40), (4.42) (4.51) and (4.52), we get the similar solution for Newtonian fluid

$$u_c(y,t) = 1 - y - 2K_{\text{eff}}Re\sum_{n=1}^{\infty}\frac{Sin(\lambda_n y)}{\lambda_n\left(\lambda_n^2+K_{\text{eff}}Re\right)} - 2\sum_{n=1}^{\infty}\frac{\lambda_n Sin(\lambda_n y)}{\lambda_n^2+K_{\text{eff}}Re}e^{-\left(\frac{\lambda_n^2}{Re}+K_{\text{eff}}\right)t}, \tag{4.53}$$

$$\tau_c(y,t) = -\frac{1}{Re} - 2K_{\text{eff}}\sum_{n=1}^{\infty}\frac{Cos(\lambda_n y)}{\lambda_n^2+K_{\text{eff}}Re} - \frac{2}{Re}\sum_{n=1}^{\infty}\frac{\lambda_n^2 Cos(\lambda_n y)}{\lambda_n^2+K_{\text{eff}}Re}e^{-\left(\frac{\lambda_n^2}{Re}+K_{\text{eff}}\right)t}, \tag{4.54}$$

$$Q_c(t) = \frac{1}{2} - 4K_{\text{eff}}Re\sum_{n=1}^{\infty}\frac{1}{\lambda_{2n+1}^2(\lambda_{2n+1}^2+K_{\text{eff}}Re)} \tag{4.55}$$

$$-4\sum_{n=1}^{\infty}\frac{1}{\lambda_{2n+1}^2+K_{\text{eff}}Re}e^{-\left(\frac{\lambda_{2n+1}^2}{Re}+K_{\text{eff}}\right)t},$$

$$u_1(y,t) = (1-y)t - 2tK_{\text{eff}}Re\sum_{n=1}^{\infty}\frac{Sin(\lambda_n y)}{\lambda_n\left(\lambda_n^2+K_{\text{eff}}Re\right)} \tag{4.56}$$

$$-2Re\sum_{n=1}^{\infty}\frac{\lambda_n Sin(\lambda_n y)}{(\lambda_n^2+K_{\text{eff}}Re)^2}\{1 - e^{-\left(\frac{\lambda_n^2}{Re}+K_{\text{eff}}\right)t}\},$$

and

$$\tau_1(y,t) = \frac{t}{Re} - 2K_{\text{eff}}t\sum_{n=1}^{\infty}\frac{Cos(\lambda_n y)}{\lambda_n^2+K_{\text{eff}}Re} \tag{4.57}$$

$$-2\sum_{n=1}^{\infty}\frac{\lambda_n^2 Cos(\lambda_n y)}{(\lambda_n^2+K_{\text{eff}}Re)^2}\{1 - e^{-\left(\frac{\lambda_n^2}{Re}+K_{\text{eff}}\right)t}\}.$$

4.6 Results and Discussion

The simple Couette flow of an incompressible hydromagnetic Maxwell fluid in the presence of a porous medium between two parallel plates with constantly increasing acceleration is addressed in this chapter. The fluid moves as a result of simple Couette flow or plate acceleration brought on by constant pressure. Analytical solutions for the velocity field, connected shear stress and volume flux are obtained using integral transform. In order to shed light on specific physical elements of the obtained results, the effect of the material elements on the motion of fluid is illustrated by graphic representation of shear stress and the velocity field i.e. for the flow induced by a simple Couette flow and constantly accelerating plate. Moreover, the similar solutions are recovered for Newtonian fluid as in the limiting case when $We \rightarrow 0$. We examine these findings in relation to variations in the Reynolds number (Re), effective parameter (K_{eff}), Weissenberg number (We), and different values of the time t.

Figure 4.1 and 4.5 represents how different values are related to Reynolds numbers (Re) i.e. $Re = 10, 20$ and 70 for $t = 1$, and $K_{\text{eff}} = 1$, for velocity and shear stress given by Eqs. (4.39), (4.40), (4.51) and (4.52), respectively. In both situations, the boundary condition is obviously satisfied since the velocity profile $u(y, t)$ drops from its maximum values to zero values and the shear stress $\tau(y, t)$ decreases in magnitude as y gets closer to 1.The Reynolds number (Re) measures the ratio of inertial forces to viscous forces in fluid flow, impacting the velocity distribution.

Figure 4.2 shows the impact of different values of K_{eff} on velocity profile $u(y, t)$ and shear stress $\tau(y, t)$ i.e for $K_{\text{eff}} = 2$, 4.3 and 6 for $t = 1$ and $Re = 20$ given by Eq. (4.39) and (4.40), respectively. As K_{eff} increases, the velocity profile decreases more steeply, indicating a stronger damping effect and shear stress starts from its maximum magnitude at $y = 0$ and approaches zero as y nears 1.

Figure 4.3 shows the impact of different values of t on velocity $u(y, t)$ and shear stress $\tau(y, t)$ i.e for $t = 4$, 6 and 9 for $K_{\text{eff}} = 6$ and $Re = 20$ given by Eqs.(4.39) and (4.40) respectively. I can be see that velocity is an increasing function at time and shear stress $\tau(y, t)$, is decreasing in magnitude with time, start negatively near $(y = 0)$ and nearing zero as $y \rightarrow 1$.

Figure 4.4 shows the effect of different values of K_{eff} on velocity and shear stress i.e for $K_{\text{eff}} = 0.6$, 0.8 and 1.5 for $t = 5$ and $Re = 20$ given by Eq. (4.51) and (4.52), respectively .The velocity $u(y,t)$ and shear stress $\tau(y,t)$ variations are shown in the graphs together with the parameter K_{eff} . Reduced resistance and smoother flow are indicated by smaller magnitudes of shear stress and a faster decrease of velocity with higher K_{eff} . Lower K_{eff} on the other hand, indicates greater resistance or connection in the system and produces larger velocity gradients and higher shear stress.

Figure 4.6 shows the impact of different values of t on velocity $u(y,t)$ and shear stress $\tau(y,t)$ i.e $t = 1$, 3 and 5 for $K_{\text{eff}} = 1$ and $Re = 20$ given by Eqs. (4.51), and (4.52), respectively. It can be seen that the velocity profile is an increasing function of time. Also, the magnitude of tangential stress is also increases by increasing time.

Figure 4.7 and 4.8 display the profile of velocity $u(y,t)$ presented by Eqs. (4.39), and (4.51) and corresponding shear stress $\tau(y,t)$ presented by Eqs. (4.40), and (4.52), respectively, for different values of We i.e. for $We = 0$ (Newtonian fluid), 2.9 , 3.9 and 5, for $t = 0, Re = 0$ and $K_{\text{eff}} = 0$. It is observed in both figures, the velocity field is an increasing function of We. Moreover , the profile of velocity for $We = 0$ (Newtonian fluid) is much smaller than the Maxwell fluid. Furthermore, magnitude of shear stress is also increasing by increasing We.

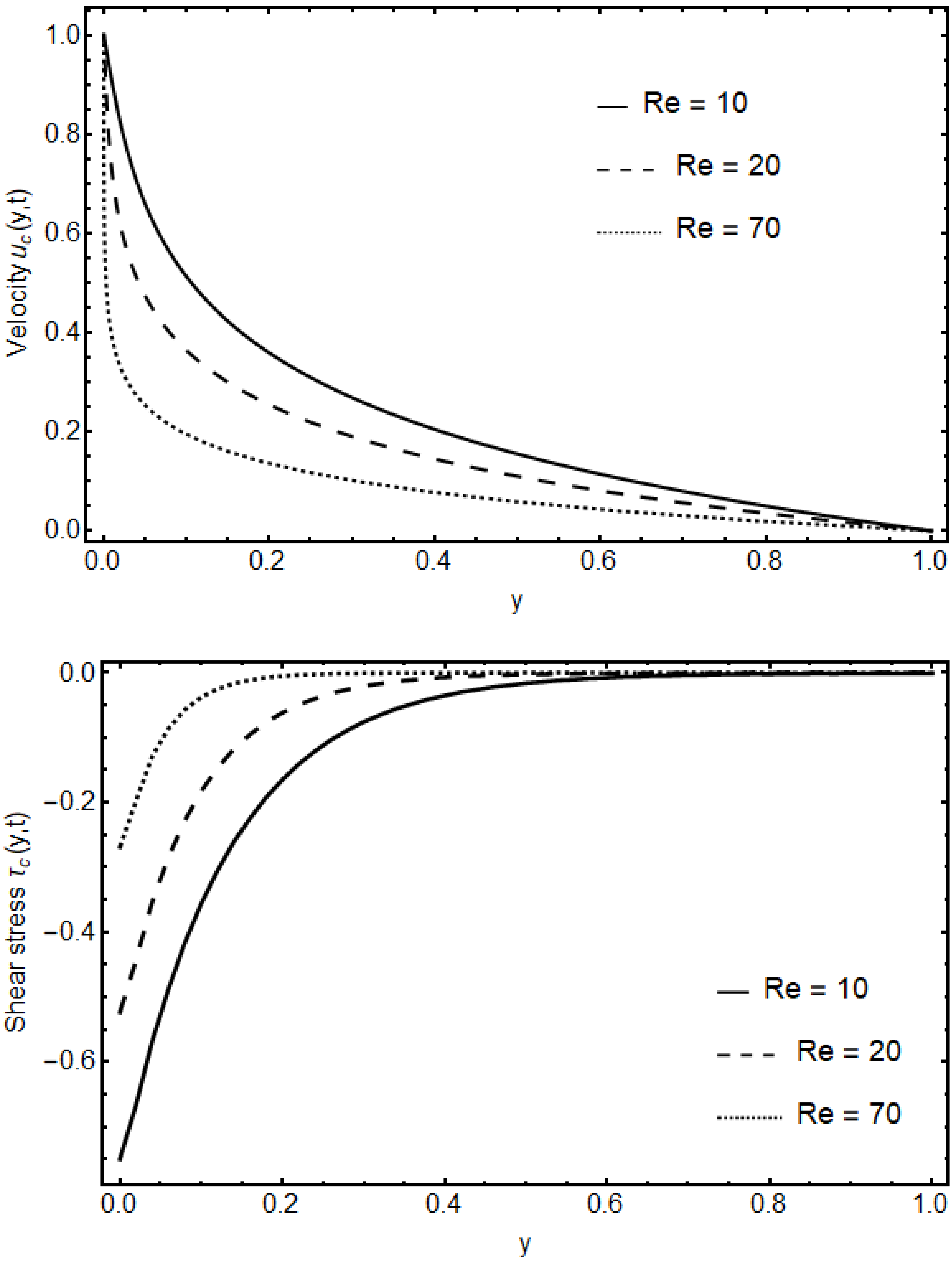

Figure 4.1: Velocity and shear stress variations for Re provided by Eqs. (4.39) and (4.40).

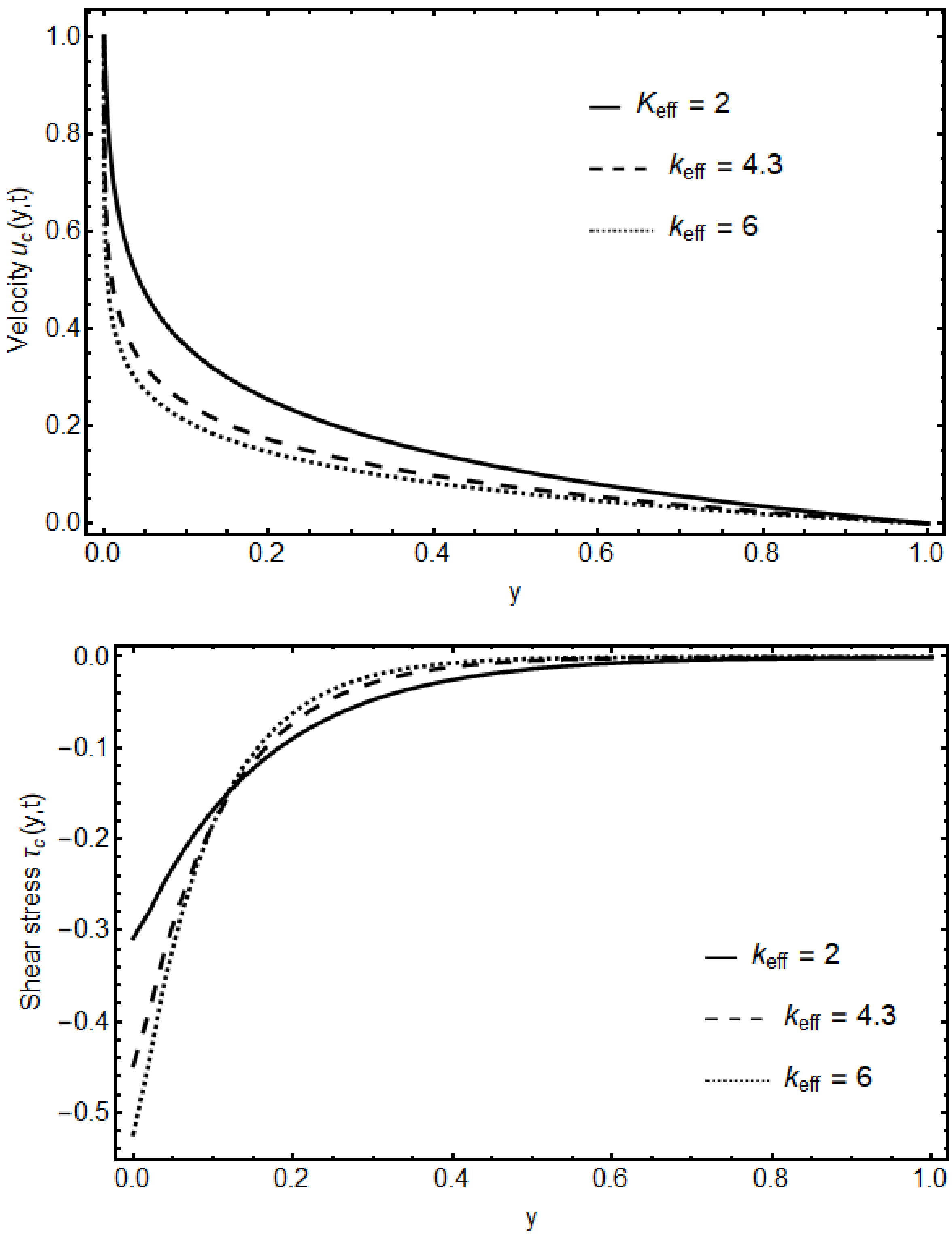

Figure 4.2: Velocity and shear stress variations for K_{eff} provided by Eqs. (4.39) and (4.40).

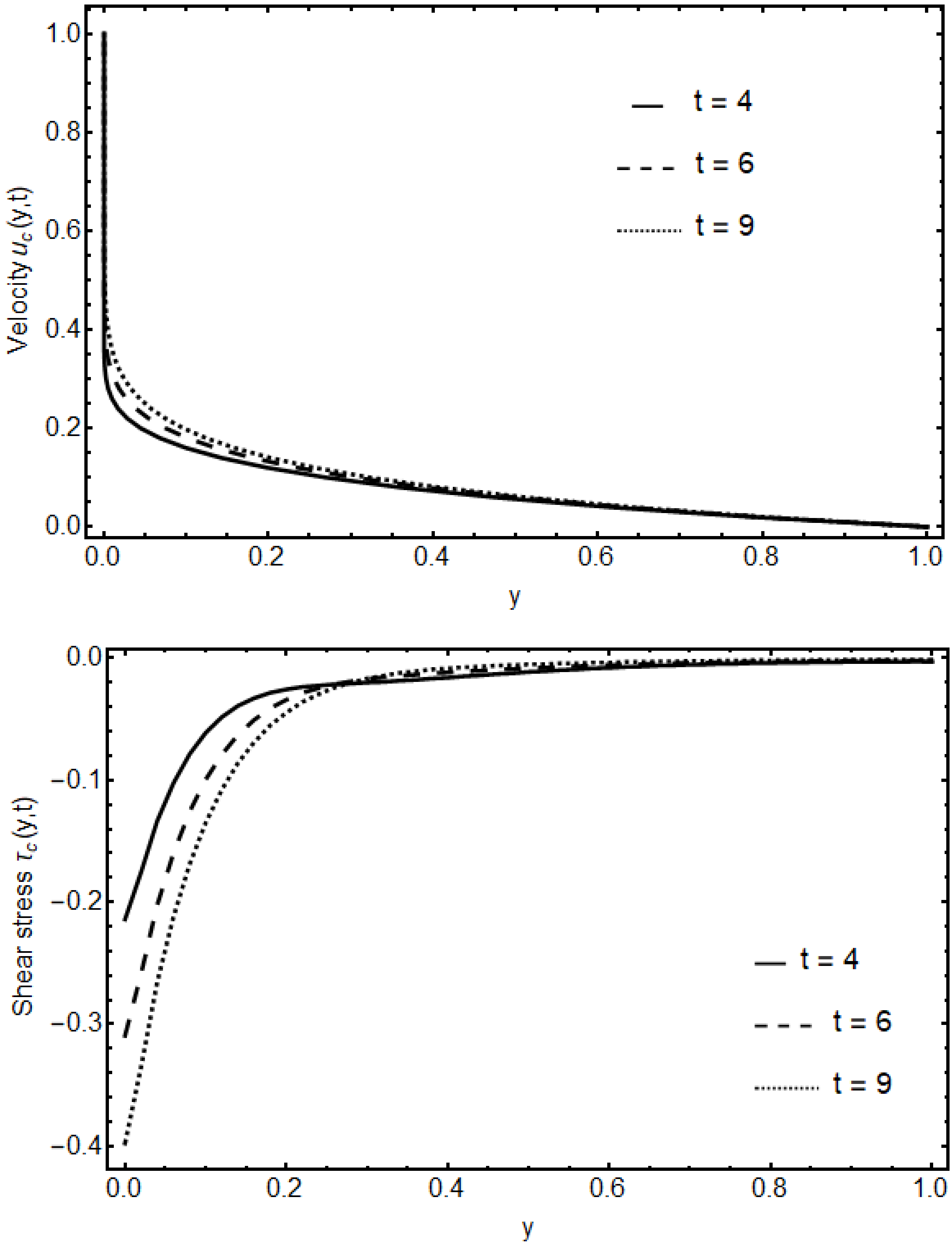

Figure 4.3: Velocity and shear stress variations for t provided by Eqs. (4.39) and (4.40).

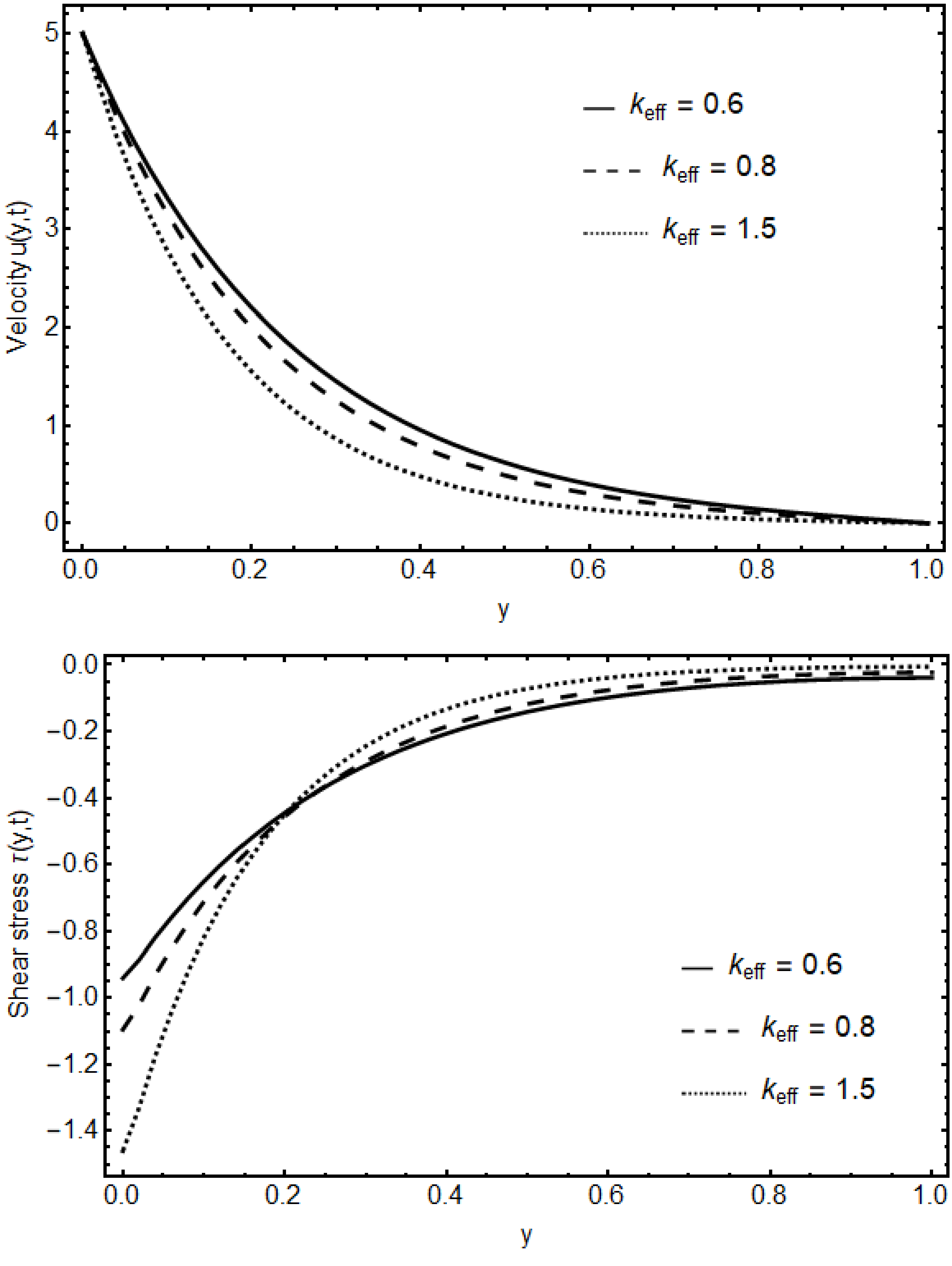

Figure 4.4: Velocity and shear stress variations for K_{eff} provided by Eqs. (4.51) and (4.52).

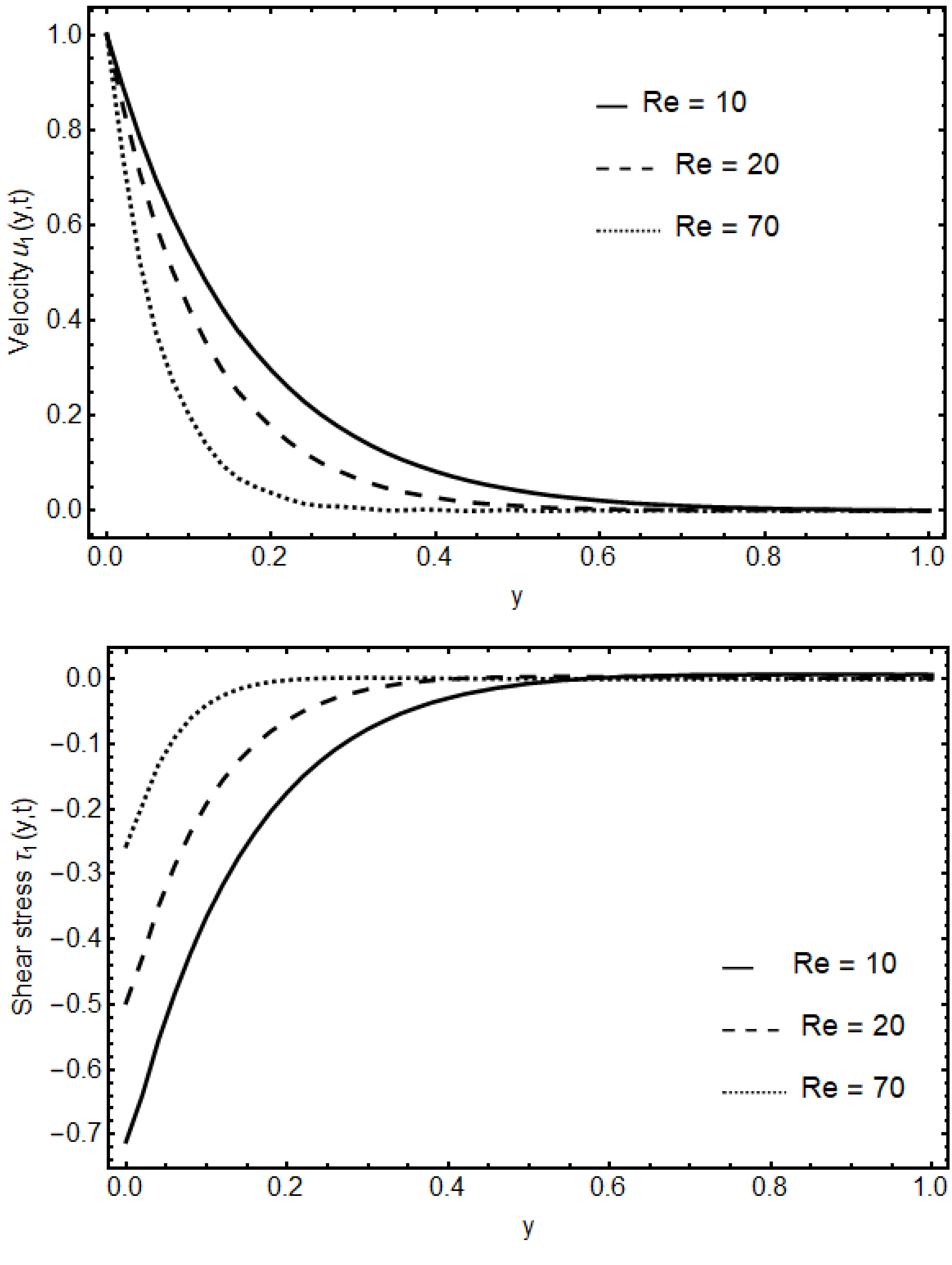

Figure 4.5: Velocity and shear stress variations for Re provided by Eqs. (4.51) and (4.52).

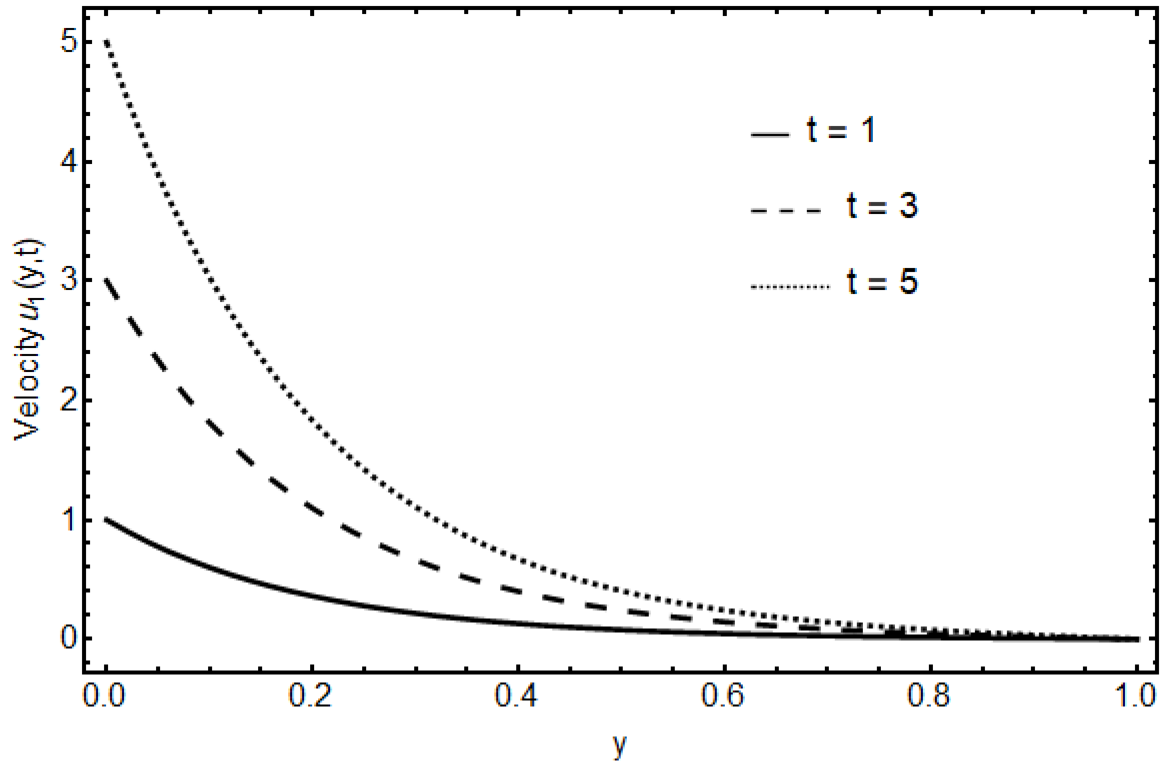

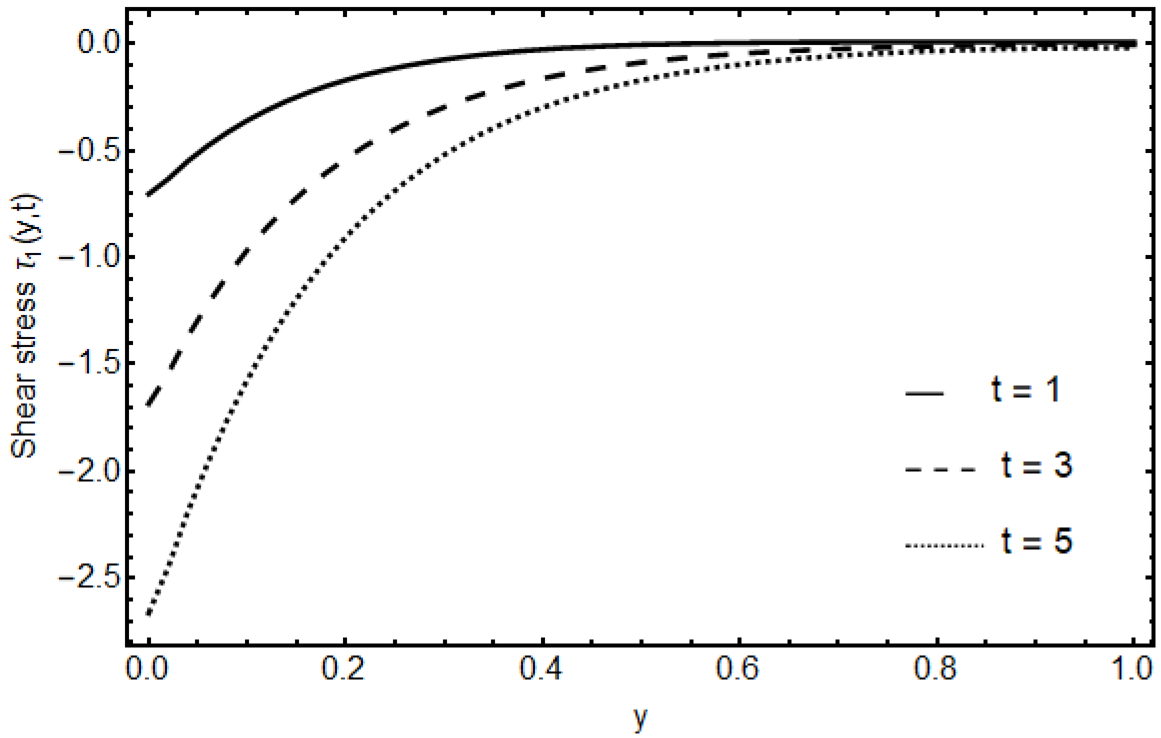

Figure 4.6: Velocity and shear stress variations for t provided by Eqs. (4.51) and (4.52).

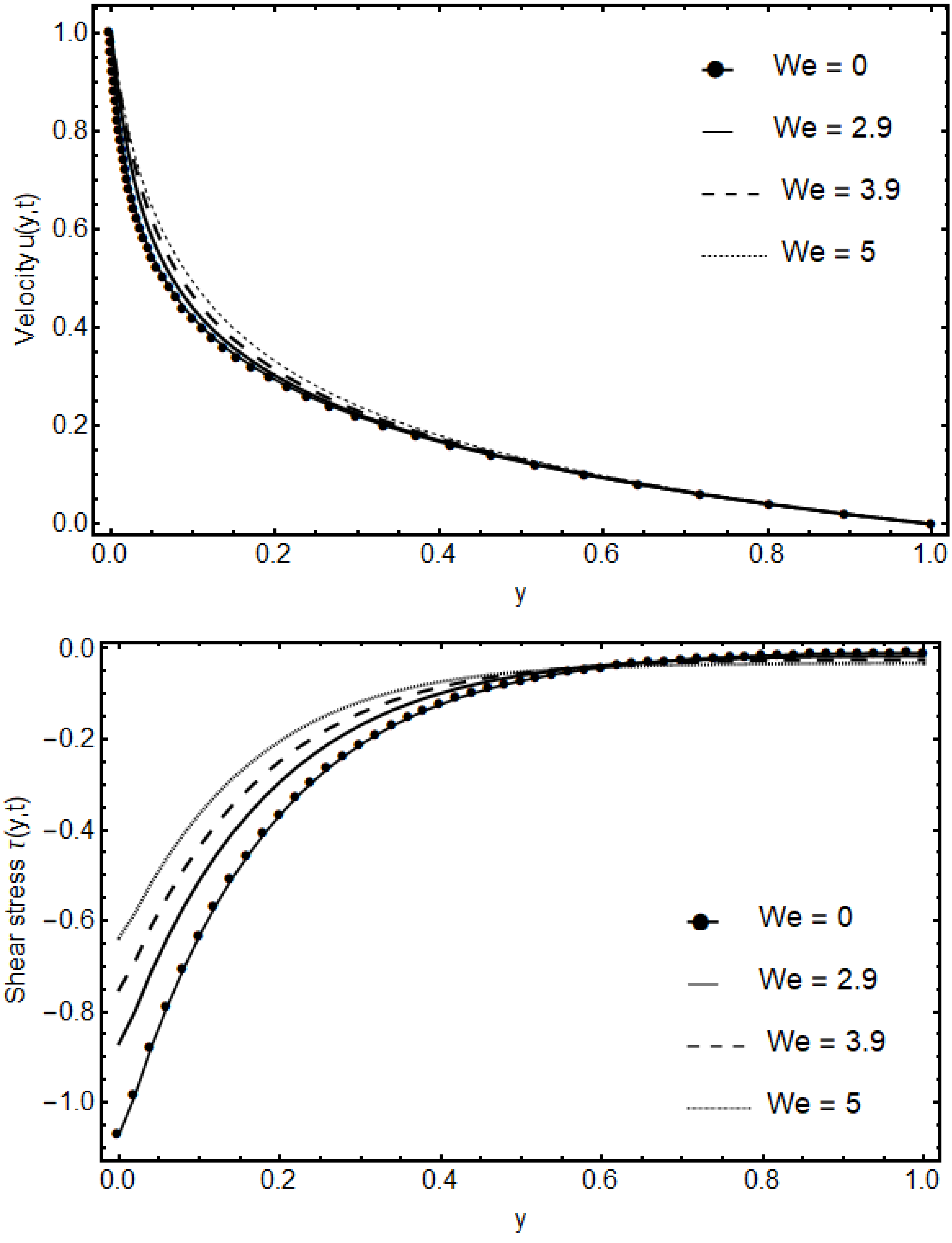

Figure 4.7: Velocity and shear stress variations for We provided by Eqs. (4.39) and (4.40).

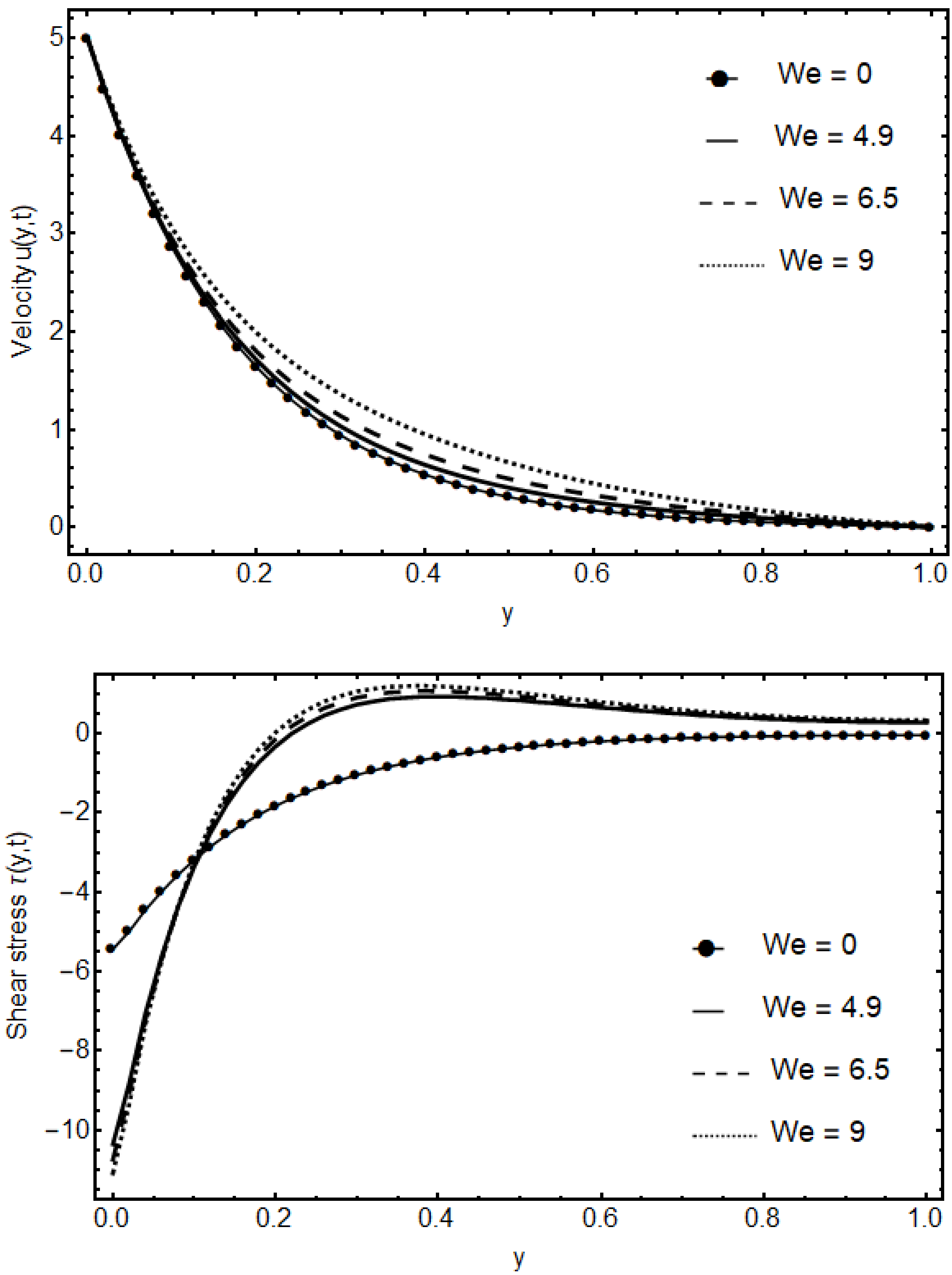

Figure 4.8: Velocity and shear stress variations for We provided by Eqs. (4.51) and (4.52).

CHAPTER 5

CONCLUSION AND FUTURE WORK

Initiating precise analytical solutions for simple Couette flow and accelerating flow of the same boundary of a non-Newtonian fluid has been the main goal of this thesis. The unsteady flows of a Newtonian fluid presented in chapter#3 and the work of chapter#3 is extended to incompressible hydromagnetic Maxwell (ch#4) and effects of porous media were taken into consideration. Integral transform is used to develop analytical solution for shear stress, velocity profiles and volume flux. Solutions, which describe fluid motion at short and large times were obtained for simple Couette flow. These solutions help identify the point at which only permanent behavior remains after temporary effects vanish. Maxwell ($We \neq 0$) and Newtonian ($We = 0$) were displayed graphically for both motion of the boundary. The major findings and contributions made by this research and presented in previous chapters (ch#3 and ch#4) are precisely summarized as follows.

In chapter 3, we have displayed the unsteady, incompressible MHD flow of viscous fluid that is placed among two horizontals, parallel plates with a porous medium present. Pressure is considered as constant and fluid motion was induced by the simple Couette flow and the accelerating bottom plate. The solutions for velocity field, shear stress and the volume flux are obtained by means of FFST, that convert the partial differential equation into ordinary motion characteristic of these two flows depend on magnetic and porous parameters $K$and M with permutation $K_{\text{eff}} = M + \frac{1}{K}$, i.e called effective permeability. The graphical illustration shows the impact of different rheological parameters of the dimensionless parameters. Fluid velocity was shown to be reduced in the presence of a magnetic field or porous media.

Lastly, we have examined the general solutions for the hydromagnetic, unsteady Maxwell fluid in the existence of porous material in chapter 4. Two parallel plates separated h apart contain an incompressible Maxwell fluid, when pressure is applied constantly. The bottom plate's simple Couette or accelerating motion created the motion in the fluid. Using the FFST, analytical solutions for the volume flow, shear stress, and dimensionless velocity field were found. All initial and boundary conditions were met by these solutions.

The main findings of the chapter are summarizing below for both simple Couette flow and accelerating flow;

- As the Reynold number Re and effective permeability K_{eff} increases, the Maxwell fluid's velocity and shear stress decrease.
- With respect to time t, both the shear stress and the velocity field increase.
- The Weissenberg number We increases with velocity and shear stress.
- The Newtonian fluid is shown to have a smaller velocity profile and shear stress than the Maxwell fluid.

5.1 Future recommendation

Future work can extend the analysis to include heat transfer effects and variable magnetic fields to explore thermal and electromagnetic influences on flow behavior. Additionally, the impact of slip boundary conditions and non-Newtonian fluid properties can be investigated for more realistic applications. Numerical simulations and experimental validations can further support the analytical findings and provide insights into complex flow regimes.

REFERENCES

[1] Rajagopal, K. R., and A. S. Gupta. "An exact solution for the flow of a non-Newtonian fluid past an infinite porous plate." Meccanica 19 (1984): 158-160.

[2] Fetecau, Constantin, and Dumitru Vieru. "Exact solutions for unsteady motion between parallel plates of some fluids with power-law dependence of viscosity on the pressure." Applications in Engineering Science 1 (2020): 100003.

[3] Asif, Muhammad, Sami Ul Haq, Saeed Islam, Ilyas Khan, and Iskander Tlili. "Exact solution of non-Newtonian fluid motion between side walls." Results in Physics 11 (2018): 534-539.

[4] Rajagopal, K. R. "A note on unsteady unidirectional flows of a non-Newtonian fluid." International Journal of Non-Linear Mechanics 17, no. 5-6 (1982): 369-373.

[5] Sun, Xuyang, Shaowei Wang, and Moli Zhao. "Oscillatory flow of Maxwell fluid in a tube of isosceles right triangular cross section." Physics of Fluids 31, no. 12 (2019).

[6] Wenchang, Tan, Pan Wenxiao, and Xu Mingyu. "A note on unsteady flows of a viscoelastic fluid with the fractional Maxwell model between two parallel plates." International Journal of Non-Linear Mechanics 38, no. 5 (2003): 645-650.

[7] Bao, Chunxu, Lin Liu, Chiyu Xie, Jing Zhu, Yufeng Quan, Siyu Chen, Libo Feng, and Liancun Zheng. "Analysis of the absorbing boundary condition for the Maxwell fluid flow over a semi-infinite plate with considering the magnetic field." Computers & Mathematics with Applications 154 (2024): 212-223.

[8] Riaz, Muhammad Bilal, Abdon Atangana, and Nazish Iftikhar. "Heat and mass transfer in Maxwell fluid in view of local and non-local differential operators." Journal of Thermal Analysis and Calorimetry 143, no. 6 (2021): 4313-4329.

[9] Zheng, Liancun, Yaqing Liu, and Xinxin Zhang. "Exact solutions for MHD flow of generalized Oldroyd-B fluid due to an infinite accelerating plate." Mathematical and Computer Modelling 54, no. 1-2 (2011): 780-788.

[10] Jalil, Mudassar, Saleem Asghar, and Shagufta Yasmeen. "An exact solution of MHD boundary layer flow of dusty fluid over a stretching surface." Mathematical Problems in Engineering 2017, no. 1 (2017): 230-7469.

[11] Rehman, Khalil Ur, Wasfi Shatanawi, and Qasem M. Al-Mdallal. "A comparative remark on heat transfer in thermally stratified MHD Jeffrey fluid flow with thermal radiations subject to cylindrical/plane surfaces." Case Studies in Thermal Engineering 32 (2022): 101913.

[12] Fetecau, Constantin, Rahmat Ellahi, and Sadiq M. Sait. "Mathematical analysis of Maxwell fluid flow through a porous plate channel induced by a constantly accelerating or oscillating wall." Mathematics 9, no. 1 (2021): 90.

[13] Fetecau, Constantin, Dumitru Vieru, and Ahmed Zeeshan. "Analytical Solutions for Two Mixed Initial-Boundary Value Problems Corresponding to Unsteady Motions of Maxwell Fluids through a Porous Plate Channel." Mathematical Problems in Engineering 2021, no. 1 (2021): 5539007.

[14] Hassan, M., M. Marin, Abdullah Alsharif, and R. Ellahi. "Convective heat transfer flow of nanofluid in a porous medium over wavy surface." Physics Letters A 382, no. 38 (2018): 2749-2753.

[15] Krishna, M. Veera, and Ali J. Chamkha. "Hall and ion slip effects on MHD rotating flow of elastico-viscous fluid through porous medium." International Communications in Heat and Mass Transfer 113 (2020): 104-494.

[16] Yang, Shuai, Liping Wang, and Shuqin Zhang. "Conformable derivative: Application to non-Darcian flow in low-permeability porous media." Applied Mathematics Letters 79 (2018): 105-110.

[17] Jordan, P. M., and P. Puri. "Exact solutions for the unsteady plane Couette flow of a dipolar fluid." Proceedings of the Royal Society of London. Series A: Mathematical, Physical and Engineering Sciences 458, no. 2021 (2002): 1245-1272.

[18] Khaled, A-RA, and Kambiz Vafai. "The effect of the slip condition on Stokes and Couette flows due to an oscillating wall: exact solutions." International Journal of Non-Linear Mechanics 39, no. 5 (2004): 795-809.

[19] Ershkov, Sergey, Evgenii Prosviryakov, and Dmytro Leshchenko. "Exact Solutions for Isobaric Inhomogeneous Couette Flows of a Vertically Swirling Fluid." Journal of Applied and Computational Mechanics 9, no. 2 (2023): 521-528.

[20] Sun, W., A. Yalcin, and M. Oberlack. "Stability of plane Couette flow with constant wall transpiration." Physical Review Fluids 9, no. 5 (2024): 053-906.

[21] C. Fetecau and M. Narahari. "General solutions for hydromagnetic flow of viscous fluids between horizontal parallel plates through porous medium." Journal of Engineering Mechanics 146, no. 6 (2020): 04020053.

[22] Dr. R.K. Bansal, "Fluid Mechanics & Hydraulic Machines," Laxmi Publications. (2005) pp. 163–165.

[23] Shahzad, Muhammad Hasnain, Sohail Nadeem, Aziz Ullah Awan, Seham Ayesh Allahyani, N. Ameer Ahammad, and Sayed M. Eldin. "On the steady flow of non-Newtonian fluid through multi-stenosed elliptical artery: a theoretical model." Ain Shams Engineering Journal 15, no. 1 (2024): 102262.

[24] Naudet, Charles J., and Matthew J. Zahr. "A space-time high-order implicit shock tracking method for shock-dominated unsteady flows." Journal of Computational Physics ,501 (2024): 1127922024.

[25] Fanelli, Francesco, and Alexis F. Vasseur. “Effective velocity and L ∞ -based well-posedness for incompressible fluids with odd viscosity.” arXiv preprint arXiv:2401.17085 (2024).

[26] Dr. Nawazish Ali Shah “Viscous Fluid Dynamic” for Scientist and Engineers, A-ONE PUBLISHER. (2011)

[27] Schlichting, H. Boundary Layer Theory; McGraw-Hill: New York, NY, USA, 1960.

[28] Fetecau, C., S. Akhter, and C. Fetecau. “Note about magnetic and porous effects on the motion of viscous fluids.” Bul. Inst. Polit. Iasi 59, no 3 (2013): 15–20.

[29] Khan, M., R. Malik, and A. Anjum. "Exact solutions of MHD second Stokes flow of generalized Burgers fluid." Applied Mathematics and Mechanics 36 (2015): 211-224.